THE JOURNAL OF PHYSICAL CHEMISTRY A

ARTICLE

pubs.acs.org/JPCA

Study of the Structural and Electronic Properties of Valproic Acid and New Derivatives Used As Anticonvulsant Agents

Nieves C. Comelli,[†] Rosana M. Lobayan,[‡] Eduardo A. Castro,[†] and Alicia H. Jubert*[,§]

[†]INIFTA, Instituto de Investigaciones Fisicoquímicas Teóricas y Aplicadas (INIFTA), Facultad de Ciencias Exactas, Universidad Nacional de la Plata, Sucursal 4, CC 16, 1900 La Plata, Bs. As. Argentina

[‡]Facultad de Ingeniería, Universidad de la Cuenca del Plata, Lavalle 50, 3400 Corrientes, Argentina

[§]CEQUINOR, Centro de Química Inorgánica, Facultad de Ciencias Exactas y Facultad de Ingeniería, Universidad Nacional de la Plata, CC 962, 1900 La Plata, Pcia de Buenos Aires, Argentina

Supporting Information

ABSTRACT: The conformational and electronic characteristics of the polar $O_9{=}C_8{-}X_{10}$ moiety in the anticonvulsant valproic acid (Vpa) drug and some of their amides and ester derivatives are analyzed at the B3LYP level using the 6-31+G(d,p) and 6-311++G(d,p) 6d,10f basis sets. Exploring the delocalization of the electron density of the $O_9{=}C_8{-}X_{10}$ moiety by means of ELF, NBO, and AIM calculations, we found that the bending away from coplanarity of the atoms in $O_9{=}C_8{-}X_{10}$ is accompanied by a three-dimensional arrangement of donor and acceptor proton units closing nearly planar pseudorings of four, five, and six members arising from stabilizing interactions around the $O_9{=}C_8{-}X_{10}$ backbone. From the structure−property relationship analysis, we explain the origin of the change in the structural parameters and atomic charges in the polar moiety.

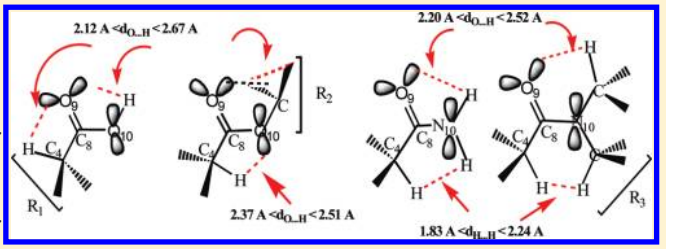

INTRODUCTION

The search for antiepileptic drugs (AEDs) with a more selective activity and lower toxicity continues to be an area of active investigation in medicinal chemistry. The current interest is due to the fact that the available AEDs suppress seizures but do not prevent the appearance of epilepsy or its progression. Moreover, they cause important central and peripheral side effects, and also, the pharmacological treatment fails to control epilepsy in up to 30% of affected people.[1]

At present, there are a large number of ligands that are marketed as AEDs due to their capacity to inhibit the sustained repetitive firing during a seizure.[1−3]

During the last two decades, several attempts have been made to develop new AED derivatives of Vpa. Tasso et al.[4] have designed novel antiepileptic ligands based on the information present in a pharmacophoric model proposed by themselves.[5] The synthesis of derivatives was planned, taking into account results of pharmacokinetic studies in simple substituted amides and esters.[6−8] In particular, the strategy used to design esters as anticonvulsant prodrugs is interesting if one considers toxicological and pharmacokinetic problems that limit the practical use of an AED.[8,9]

Regarding the structural characteristics of the derivatives reported in ref 4, all of them have a polar moiety comprising two closely located hydrogen donor−acceptor groups bonded to an sp^3-hybridized atom of a hydrophobic moiety (R_1) with a minimum of lipophilicity (two hydrophobic tails with three atoms of carbon for each one; valproyl group) and an acyl substituent R_2 of variable size but limited to the fact that the steric repulsions between R_1 and R_2 are minimized.

The in vitro activity of the derivatives designed by Tasso et al.[4] were studied via the experimental anticonvulsant maximal electroshock (MES) and subcutaneous pentylenetetrazol (PTZ) tests. The functional changes introduced in the molecule of Vpa led to active compounds in the MES test and inactive tests in the PTZ test. These findings lead to the new derivatives with a profile similar to that of pharmacophore Phenytoin (PHE-like profile), which is effective in generalized seizures by blocking voltage-dependent sodium channels. In descending order of their power to suppress induced seizures (PI = antiMES protection index), the following was reported from experimental results: 4-(valproylamido) benzenesulfonamide (Suvpd) [PI = 19] > *N*-cyclohexylvalpromide (Chvpd) [PI = 17] > *N*-ethylvalpromide (Etvpd) [PI = 5] > dimethylvalpromide (Dmvpd) [PI = 2.9] ≅ valpromide (Vpd) [PI = 2.9] > *N*-isopropylvalpromide (Ipvpd) [PI = 2.6] > valproic acid (Vpa) [PI = 2.9].

The improved protection indices in Suvpd, Chvpd, and Etvpd show these derivatives as better potential antiMES drugs than their Vpa and Vpd precursors.

From findings that validate the antiMES pharmacophoric model,[5] new derivatives of Vpa were synthesized employing bulky acyl groups, in some cases with polar and aryl groups next to the region O=C—O/N: *N*-alphafenetylvalpromide (Aphvpd), *N*-benzhydrylvalpromide (Bzvpd), *N*-ethylaminevalpromide (Etavpd), 1-isobutanol valproate (Isbvpa), 1-secbutanol valproate (Secbvpa), isopentyl

Received: August 29, 2010
Revised: December 7, 2010
Published: February 10, 2011

valproate (Ispvpa), and benzyl valproate (Benvpa). In these molecules, structural changes in Vpa and Vpd provide the inclusion of functional groups considered essentials in other pharmacophoric models for antiMES activity.[10,11] In addition, we note that the new derivatives exhibit stereoelectronic features according to new requirements reported by Gavernet et al.[12] for antiMES activity obtained using three-dimensional models of comparative molecular field analysis (3D-CoMFA).

The origin of the biological activity of derivatives of Vpa and the interpretation of the regulating factors were investigated from quantitative structure−activity relationship models (QSAR) using different molecular descriptors.[13−15] In these reports, the importance of the electronic properties of the C═O group and adjacent atoms in controlling the anticonvulsant behavior was pointed out. From these findings, it is postulated that the manifestation of the activity of Vpa and its derivatives involves initial electrostatic interactions between the C═O group and the receptor active site.

From these results and based on the consideration that the receptor site perceives an approaching electronic distribution, as well as that molecules with similar biological activity share certain physicochemical characteristics, we propose here to explore the structural and electronic change on the polar region of the novel derivatives of Vpa presented above.

The quantum mechanical description of the structural and electronic properties of the Vpa and derivatives was obtained by means of the natural bond orbital (NBO) approach,[16] with the electron localization function (ELF)[17] and quantum theory of atoms in molecules (AIM)[18] analysis. We present a systematic study of the equilibrium structures and the electronic and topological properties of the polar R_1—C_8(═O_9)—$X_{10}R_2R_3$ fragment [where R_1 = —CH—(CH_2—CH_2—CH_3)$_2$; X_{10} = O, N; R_2 = —H, —CH_3, —CH_2—CH_3, —CH—(CH_3)$_2$, —(CH_2)$_2$—CH_3, —(CH_2)$_2$—CH(CH_3)$_2$, —C_6H_{11}, —(CH_2)$_2$—NH_2, —C(CH_3)·OH—CH-(CH_3)$_2$, —CH·OH—CH(CH_3)$_2$, —CH_2—(C_6H_5), —CH-(CH_3)(C_6H_5), —CH—(C_6H_5)$_2$, and —C_6H_4·SO_2·NH_2; and R_3 = H and —CH_3, lp (lone pair electrons)].

From a comparative study of the electronic effects of the substituent on the electron distribution in the polar region, we propose some new alternative insights for the interpretation of the activity in Suvpd, Chvpd, Etvpd, Dmvpd, Vpd, Ipvpd, Prvpa, and Vpa that allow us to predict the antiMES activity of Aphvpd, Bzvpd, Etavpd, Secbvpa, Isbvpa, Ispvpa, and Benvpa and design new antiMES ligands from the Vpa.

COMPUTATIONAL METHODS

The molecular structures of all of the Vpa derivatives were built by means of Hyperchem software.[19] The conformational space of Vpa and its derivatives was investigated using molecular dynamic simulations and the MM+ force field available in this software.

The starting geometries were generated by heating from 0 to 900 K in 0.1 ps. The temperature was kept constant by coupling the system to a thermal bath with a relaxation time of 0.5 ps. A 500 ps long simulation was performed after an equilibration period of 10 ps, saving molecular Cartesian coordinates every 10 ps. The time step for the simulations was 0.1 fs. Outcome geometries were then optimized to an energy gradient less than 0.001 kcal·mol^{-1} Å^{-1} using the semiempirical method AM1 also implemented in the Hyperchem package.

We have performed a full geometry reoptimization of the conformers obtained according to the above methodology, and the minima were characterized through their vibrational analyses. We have employed the force gradient Bernys algorithm method,[20] the hybrid GGA method B3LYP,[21,22] and the medium-size basis set 6-31+G** as implemented in the Gaussian 03 package.[23] NBO calculations were performed using the 6-311++ G**(6d,10f) basis set and the NBO 3.1 code[24] as implemented in Gaussian 03.

The ELF[25] function analysis has been done with the TOPMOD package,[26] and AIM analysis was performed with the AIMPAC package[27] using wave functions obtained from Gaussian 03 at the same level of theory of NBO calculations.

RESULTS AND DISCUSSION

A. Structural Analysis. The structure of the molecules studied is shown in Figure 1.

Because there is not up to ddate available information in the literature over X-ray diffraction data of Vpa, esters, and N-mono and N,N-disubstituted derivates of Vpa, in Table 1, we report the theoretically predicted structural parameters of the polar fragment (O_9═C_8—X_{10}). In Table 1S (see Supporting Information) we summarize additional structural data of these molecules corresponding to the bond lengths and angles of the different substituents bonded to the polar moieties (O_9═C_8−O_{10} and O_9═C_8−N_{10}).

According to our calculations, the lowest-energy conformers of Vpa and derivatives belong to the C_1 symmetry point group. The O_9═C_8—X_{10} fragment exhibits a syn conformation [$-8.1° \leq \delta_{O9═C8—X10—C/H} \leq 3.7°$], and while in the amides and esters the $\delta_{H—C4—C8═O9}$ dihedral angle presents an anti configuration [$|162.2°| \leq \delta_{H—C4—C8═O9} \leq |179.9°|$], in the Vpa, the $\delta_{H—C4—C8═O9}$ angle presents the syn configuration ($\delta_{H—C4—C8═O9}$=0°).

Calculation of polarizability ⟨α⟩ (see Table 1) was performed from $\langle\alpha\rangle = (1/3)(\alpha_{xx} + \alpha_{yy} + \alpha_{zz})$, where the tensor components are obtained from the second derivatives of the energy with respect to the Cartesian components of the applied electric field ε ($\alpha = [\partial^2 E/\partial\varepsilon^2]$). Considering the value of polarizability, we observed that this property changes, in agreement with the factors that regulate the polarization of the electronic distribution in a chemical system.[28] In fact, while less polarizable molecules [α < 155.3 au] have small substituents with a low effective nuclear screening (Vpa, Vpd, Dmvpd, Etvpd, Prvpa, Etavpd, Ipvpd, Secvpa, Isbvpa), more polarizable derivatives [α > 155.3 au] present large alkyl substituents of low electronegativity (Ispvpa, Chvpd) or a moiety with conjugated bonds (aryl groups: Benvpa, Apvpd, Suvpd, and Bzvpd).

With respect to the structural and chemical properties of the polar moiety, the classical interpretation indicates that they are dominated by the electronegativity of O_9 and the interaction of the lp_{X10} with the $C_8^{\delta+}$.[29] With a lp_{X10} in its minimum of energy, the bonds scheme indicates a planar backbone with a polarized C_8═O_9 bond and a C_8—X_{10} bond with partial double bond character related to the $^{\delta-}O_9$—C_8:::$X_{10}^{\delta+}$ resonant form. This model offers an adequate explanation for the existence of isomers Z/E around the C_8—X_{10} bond and the chemical stability of the carboxylate/amide group in nucleophilic/electrophilic substitution reactions. Distortions of the planarity, pyramidization of C_8 and X_{10}, and reduction of the rotational barrier around the C_8—X_{10} bond are associated with a O_9═C_8—N_{10} resonant form.

Because a substituent is a structural unit which influences the properties of the molecule in a quantitative sense but does not alter its general character,[30] we have evaluated the change in the geometry of the polar portion when the H atom in —OH or —NH (Vpa or Vpd) is replaced by the substituents identified earlier.

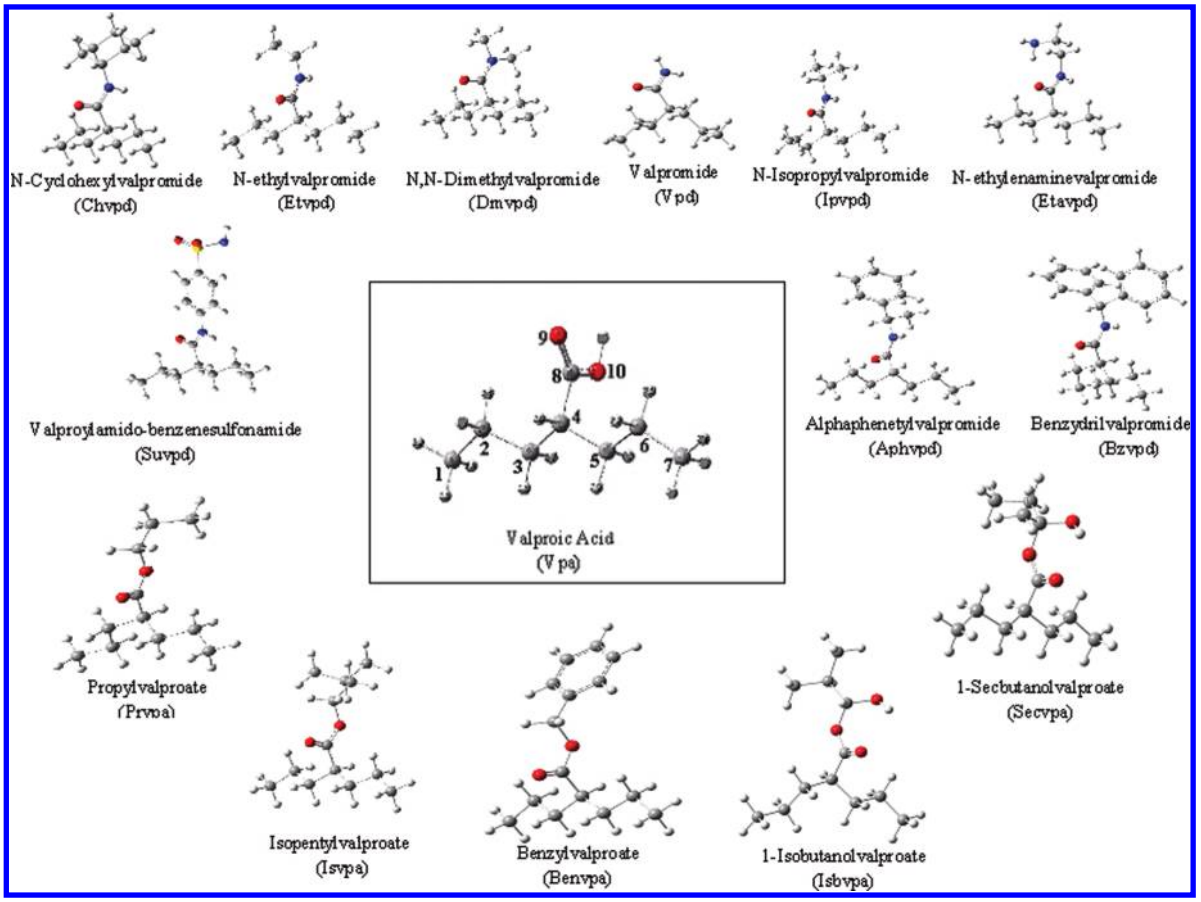

Figure 1. The lowest-energy conformers of valproic acid and derivatives selected for this study. The numbering corresponds to the atoms of the valproyl moiety, which is the same for all of the structures.

Table 1. Relevant Structural Parameters (r and δ) of the Molecules in the Polar Regions and Polarizability ($\langle\alpha\rangle$) Calculated at B3LYP/6-31+G[a]**

parameters	Vpa	Aphvpd	Bzvpd	Chvpd	Dmvpd	Etavpd	Etvpd	Ipvpd	Suvpd	Vpd	Benvpa	Ispvpa	Prvpa	Isbvpa	Secvpa
$r_{C4—H}$	1.096	1.1	1.099	1.101	1.094	1.1	1.1	1.099	1.1007	1.1	1.096	1.096	1.095	1.096	1.096
$r_{C4—C8}$	1.518	1.533	1.532	1.534	1.537	1.534	1.534	1.534	1.532	1.534	1.522	1.523	1.522	1.519	1.522
$r_{C8=O9}$	1.214	1.232	1.23	1.232	1.235	1.231	1.228	1.232	1.225	1.224	1.217	1.217	1.216	1.223	1.225
$r_{C8—X10}$	1.362	1.365	1.371	1.365	1.377	1.369	1.368	1.370	1.383	1.367	1.353	1.352	1.353	1.348	1.343
$r_{X10—H}$	0.972	1.01	1.011	1.0092		1.009	1.009	1.010	1.010	1.006					
$\delta_{H—C4—C8=O9}$	0	−179.7	−169.5	179.1	178.1	176.2	−179.9	−178.8	−179.5	169.7	179.9	178.6	−162.2	−166.5	−175.3
$\delta_{O9=C8—X10—(H/C)}$	0	2.7	−8.1	1.5	0.5	3.7	−2.9	1.8	0.4	−1.1	0	0.4	−1.2	−3.4	0.9
$\langle\alpha\rangle$	102.6	199.3	254.5	174	131.3	141	131.4	142.7	219.5	107.6	183.6	162.5	138.8	155.3	153.9

[a] Distances in Å, angles in degrees, and polarizability in au.

For a quantitative description of the degree of distortion of planarity of the polar moiety, we calculated the parameters of the Winkler−Dunitz τ, χ_C, and χ_X, which represent the twisting around the $C_8—X_{10}$ bond (τ) and the pyramidal out-of-plane deviations on the carbonyl carbon and X_{10} atom (χ_C and χ_X). These parameters were calculated from the internal coordinate set and the relationship shown in Figure 2, as described elsewhere.[31] Internal coordinates w_1 and w_2 for Vpa and its derivatives were calculated according to the procedure detailed in ref 32 using the Cartesian coordinates of the atoms and the electron lone pair in the $O_9{=}C_8—X_{10}$ backbone obtained from the structural information given by the ELF calculation.

In Table 2 are gathered the values of the geometrical parameters describing the out-of-plane distortion of the $O_9{=}C_8—X_{10}$ along with the percentage of changes of $r_{C8=O9}$ and $r_{C8—X10}$ ($\%\Delta r_{C8—X10}$ and $\%\Delta r_{C8=O9}$, respectively) calculated from

$$\%\Delta r = \frac{r(\tau) - r(\tau \approx 0)}{r(\tau \approx 0)} \times 100$$

The $r(\tau{\approx}0)$ values correspond to $r_{C8—X10}$ and $r_{C8=O9}$ from the less distorted $O_9{=}C_8—O_{10}$ and $O_9{=}C_8—N_{10}$ groups (Benvpa and Aphvpd).

According to our calculations, values of τ in the range $[0.01°;4.5°]$ indicate that the $O_9{=}C_8—X_{10}$ group is slightly nonplanar. Regarding the changes of τ with the different substituents, in Table 2, it is shown that while important distortions induced by the bulky —CH—$(CH_2—CH_2—CH_3)_2$ substituent in Vpa and Vpd are compensated in the carboxylate group by bulky

dx.doi.org/10.1021/jp1081998 |J. Phys. Chem. A 2011, 115, 1686–1700

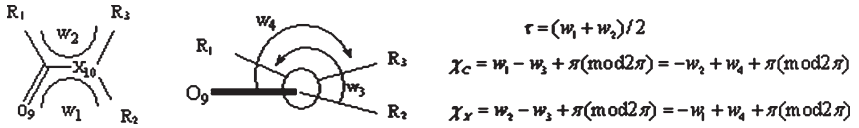

Figure 2. The four dihedral angles used for determining the torsional angle τ and the pyramidicity descriptors χ_C and χ_X.

Table 2. Descriptors of the out-of-Plane Deformation in $R_1—C_8(=O_9)—X_{10}R_2R_3$ and $\%\Delta r_{C8—X10}$ and $\%\Delta r_{C8=O9}$ Calculated Using As Reference Values of the $r_{C8—X10}$ and $r_{C8=O9}$ of Molecules with the $O_9=C_8—X_{10}$ Group Less Distorted in the Gas Phase[a]

molecules	τ(°)	χ_C(°)	χ_X(°)	$\%\Delta r_{C8—X10}$	$\%\Delta r_{C8=O9}$
			$O_9=C_8—O_{10}$		
Benvpa	0.01	0.01	0.02	0	0
Ispvpa	0.4	0.2	1.8	−0.1	0
Secvpa	0.94	1.06	4.73	−0.75	0.66
Prvpa	1.25	2.08	2.02	−0.02	−0.04
Isbvpa	1.74	1.76	5.15	−0.38	0.5
Vpa	4.55	0	9.1	0.62	−0.21
			$O_9=C_8—N_{10}$		
Aphvpd	0.3	0.1	5.9	0	0
Suvpd	0.48	0.04	−0.19	1.32	−0.54
Bzvpd	0.5	0.6	15.9	0.44	−0.18
Etvpd	0.9	−0.7	6.7	0.22	−0.36
Etavpd	1.1	0.7	5.9	0.32	−0.12
Dmvpd	1.2	−0.3	3.1	0.89	0.19
Chvpd	1.28	−1.43	−0.92	0.01	−0.01
Ipvpd	1.55	−1	5.7	0.07	−0.03
Vpd	2.25	2.2	−4.5	0.18	−0.66

[a] Angles are in degrees, and distances are in Å. Data reported were obtained at the B3LYP/ 6-311++G**(6d,10f) level and presented in increasing order of τ.

substituents such as $—CH_2—(C_6H_5)$, $—(CH_2)_2—CH(CH_3)_2$, and $—C(CH_3)\cdot OH—(CH_2)_2—CH_3$, the amide moiety is more planar when it is linked to substituents $—CH(CH_3)(C_6H_5)$, $—C_6H_4—SO_2NH_2$, and $—CH—(C_6H_5)_2$. Substituents like $—(CH_2)_2—CH_3$, $—CH(OH)—CH(CH_3)_2$, $—CH_2—CH_3$, $—CH_2—CH_2—NH_2$, $—CH_3$, $—C_6H_{11}$, and $—CH(CH_3)_2$ control only partially the distortion in $O_9=C_8—X_{10}$.

Regarding the values of χ_C and χ_X angles, while an increase of τ is accompanied by nonregular changes of χ_C and χ_X, it can be seen from Table 2 that the pyramidalization on the X_{10} atom ($0 < \chi_X < 15.9°$) is higher than the indicated on the C_8 atom ($0 < \chi_C < 2.2°$).

To describe how the distortion of the planarity in the polar moiety proceeds, we assume that the O_9, C_{R1}, C_{R2}, and R_3 units are defining a reference plane, as can be seen in Figure 3. From data in Table 2, the change of substituents in this region defines combinations between the w_1, w_2, w_3, and w_4 angles (Figure 2), which leads to a polar backbone that is (1) planar with all atoms coplanar, (χ_C and $\chi_X < 1°$; Figure 3a; Benvpa, Suvpd) or (2) slightly distorted from planarity, where (a) only the X_{10} atom deviates from the coplanarity ($\chi_C < 1°$ and $\chi_X > 1°$, Ispvpa, Vpa, Aphvpd, Bzvpd, Etvpd, Etavpd, and Dmvpd; Figure 3b), (b) both C_8 and X_{10} deviate to the same side of the reference plane (Secvpa, Prvpa, Isbvpa, and Chvpd; Figure 3c), or (c) both C_8 and X_{10} deviate from the coplanarity but in opposite directions with respect to the reference plane (Ipvpd and Vpd; Figure 3d).

Results of Table 2 show that in esters, the $\%\Delta r_{C8=O9}$ and $\%\Delta r_{C8—X10}$ values and their relationship with τ values present a tendency of change $\%\Delta r_{C8—X10} < 0$ and $\%\Delta r_{C8=O10} > 0$ as τ increase. This behavior indicates that the most planar carboxylate backbone (Benvpa, $\tau = 0.01°$) does not show the shortest $C_8—O_{10}$ and largest $C_8=O_9$ bonds, respectively, as expected when considering the Pauling model. Taking into account the structural data from Table 1, it can be seen that the carboxylate group with the most polarizable π system corresponds to the Secvpa where $\tau = 0.94°$.

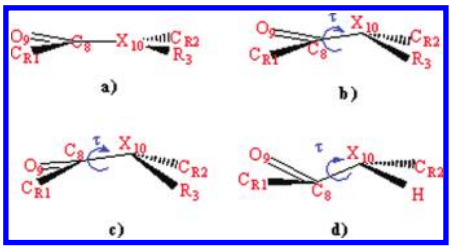

Figure 3. Enlarged side view of C—X bonds displaying the type of distortion identified for the O=C—X core in Vpa and its derivatives. C_{R1} and C_{R2} = atoms, whereas the R_1 and R_2 are substituents linked to the polar moiety.

In amides, although Aphvpd is the molecule with the less distorted amide backbone and with the shortest $C_8—N_{10}$ bond (Table 2), it does not show the largest $C_8=O_9$ bond. In Suvpd, where the polar region is slightly distorted, we find the largest $\%\Delta r_{C8—X10}$ and $\%\Delta r_{C8=O9}$.

From our observations, we consider that molecules with short $C_8—X_{10}$ and large $C_8=O_9$ bonds cannot be associated with a $^{\delta-}O_9—C_8:::X_{10}^{\delta+}$ resonant form because they do not have a planar polar group; on the other hand, molecules with large $C_8—X_{10}$ and short $C_8=O_9$ bonds cannot be represented by a $O_9=C_8—N_{10}$ resonant form because they do not have the polar region more distorted.

We believe that the nonregular behavior of τ, χ_C, χ_X, $\%\Delta r_{C8=O9}$, and $\%\Delta r_{C8—X10}$ when the substituent of the X_{10} atom is changed ($H \rightarrow R_2$) indicates that our results do not support the Pauling resonance model arguments. In fact, from the nondependence of $r_{C8—X10}$ and $r_{C8=O9}$ with the twisting around the $C_8—X_{10}$ bond and the C_8 and X_{10} pyramidalization, we infer that in the polar moiety, there is a complex electronic distribution that, due to the steric effect of R_1 and R_2 on the C_8 and X_{10} atoms, cannot be explained by taking into account only the loss of the $2p_z$ unshared delocalization of the lp_{X10} on the π-system.

B. Natural Charges Analysis. Looking for more evidence to the above interpretation, we consider it important to examine the nature of the interaction of R_1, R_2, and the atom X_{10} with the group $C_8=O_9$ in Vpa and its derivatives. Using wave functions at the B3LYP/6-311++G**(6d,10f) level, we summarize in Table 3 the charge distribution in the polar region and the adjacent atoms together with the charge of the lp_{X10} that delocalizes in the $\pi^*_{C=O}$ ($n_{X10} \rightarrow \pi^*_{C=O}$) calculated using the NBO method.

From Table 3, it can be seen that the bioisosteric replacement of —OH by $—NH_2$ increases the natural charge values on the O_9 and X_{10} atoms and decreases the natural charge on C_8. The substitution of a H atom by alkyl substituents in the polar moiety increases the natural charge values on the O_9 and C_8 atoms and

Table 3. Natural Charge Distribution on O_9═C_8—N_{10} and Atoms of R_1 and R_2 Adjacent to the Polar Region Together with the $n_{X10} \rightarrow \pi^*_{C=O}$ Charge Calculated at the B3LYP/6-311++G(6d,10f) Level[a]**

molecules	Q_{CR1}[b]	Q_{C8}	Q_{O9}	Q_{O10}	Q_{CR2}[b]	$n_{X10} \rightarrow \pi^*_{C=O}$
			O_9═C_8—O_{10}			
Benvpa	−0.291	0.802	−0.607	−0.547	−0.057	0.221
Ispvpa	−0.291	0.803	−0.608	−0.559	−0.041	0.225
Secvpa	−0.291	0.819	−0.647	−0.581	0.572	0.247
Prvpa	−0.292	0.806	−0.605	−0.562	−0.040	0.217
Isbvpa	−0.293	0.818	−0.638	−0.565	0.423	0.217
Vpa	−0.298	0.791	−0.589	−0.696	0.218	0.198
			O_9═C_8—N_{10}			
Aphvpd	−0.275	0.671	−0.650	−0.627	−0.045	0.285
Suvpd	−0.277	0.679	−0.615	−0.596	0.171	0.320
Bzvpd	−0.281	0.680	−0.641	−0.623	−0.069	0.299
Etvpd	−0.277	0.668	−0.646	−0.629	−0.198	0.304
Etavpd	−0.276	0.665	−0.647	−0.636	−0.214	0.367
Dmvpd	−0.279	0.679	−0.654	−0.494	−0.354	0.009
Chvpd	−0.275	0.670	−0.649	−0.640	−0.033	0.348
Ipvpd	−0.282	0.670	−0.649	−0.632	−0.040	0.254
Vpd	−0.279	0.663	−0.629	−0.801	0.186	0.254

[a] The sequence of molecules is arranged in ascending order of τ, and the values of the charges are in au. [b] Subscript R1 indicates an atom of the valproyl moiety, and subscript R2 indicates an atom of the acyl substituent vicinal to the polar region.

decreases the natural charge values on X_{10}. In amides, an exception to the increase of Q_{O9} with the functionalization to secondary amide is indicated in Suvpd. In this structure, $Q_{O9,Vpd} > Q_{O9,Suvpd}$.

Although in a Benvpa molecule, where the carboxylate moiety is planar, we found the lowest values of Q_{O10}, an O_9 and C_8 with the highest natural charge and a highest delocalization $n_{X10} \rightarrow p^*_{C=O}$ are not found. In Secvpa (with τ = 0.94°), the natural charge on O_{10} and C_8 and the $n_{X10} \rightarrow \pi^*_{C=O}$ delocalization are the highest of the series. The low values of charges on the O_9 and C_8 atoms in Vpa along with a reduced $n_{X10} \rightarrow \pi^*_{C=O}$ delocalization indicate a carboxylate moiety mainly formed by the C_8═O_9 and C_8—O_{10} bonds.

From these observations, although it is not possible to associate the planar carboxylate group of the derivatives of Vpa to the electronic distribution $^{\delta-}O_9$—C_8:::$O_{10}{}^{\delta+}$, for the Vpa, it seems appropriate to consider an electron distribution on the polar region according to the O_9═C_8—O_{10} resonant form because it has the shortest C_8═O_9 and the largest C_8—C_{10} bonds of all of the carboxylic derivatives under study.

Considering the electronic distribution in amide moieties where τ < 1°, although Q_{O9} in Aphvpd (−0.650 au) is very close to the most negative value observed in amides, in this molecule, it is not found for the N_{10} atom with minor negative charge and the highest $n_{X10} \rightarrow \pi^*_{C=O}$ value. In contrast, in structures where τ >1° and the highest value of $n_{X10} \rightarrow \pi^*_{C=O}$ (0.367 au in Etavpd and 0.348 au in Chvpd) is predicted, the charges on O_9 and N_{10} do not allow us to recognize this region with an electronic distribution of the type $^{\delta-}O_9$—C_8:::$N_{10}{}^{\delta+}$. The more distorted polar region (Vpd), which shows a reduced natural charge on O_9 and C_8, low $n_{X10} \rightarrow \pi^*_{C=O}$ delocalization, and a high charge density on N_{10} could not be related to the O_9═C_8—N_{10} resonant form because it does not have the largest C—N bond of the whole series of amides under study.

On the other hand, taking into account the way Q_{CR1} and Q_{CR2} change with Q_{O9}, Q_{C8}, and Q_{O10}, the arrangement of structures in increasing order of τ allowed us to recognize the following regularities (Table 3).

In the carboxylate group

(i) Q_{CR1} decreases slightly with the increase of the electronegative or electropositive character of R_2 (Q_{CR2} is the most negative or the most positive).

(ii) Atoms are coplanar when R_2 is electronegative (Benvpa) or very electropositive (Secvpa).

(iii) Q_{C8} decreases to some extent when R_2 electronegativity increases.

(iv) The polarity of C_8═O_9 and C_8—X_{10} increases slightly with the electron-donor character of R_2 (when Q_{CR2} is more positive, $|Q_{C8}|$, $|Q_{O9}|$, and $|Q_{X10}|$) are larger, and they diminish if R_2 is electronegative (i.e., when Q_{CR2} is more negative, then one obtains slightly low values of $|Q_{C8}|$, $|Q_{O9}|$, and $|Q_{X10}|$.

(v) Regarding $n_{O10} \rightarrow \pi^*_{C=O}$ values, we can see that they are relatively high if R_2 is very electropositive (Secvpa). On the contrary, we cannot note a well-defined relationship between $O_{10} \rightarrow \pi^*_{C=O}$ and the change of electronegativity in R_2 (Benvpa, Prvpa).

In the amide function, although there is not a clear change relationship between Q_{CR1} and Q_{CR2}, the R_2 electronic effects are related to the Q_{O9}, Q_{C8}, and Q_{O10} values, and they show an inverse behavior to that shown for carboxylic compounds.

(i) The electronic distribution is asymmetric, and the C_8═O_9 and C_8—N_{10} bond polarities are relatively low when an R_2 moiety is rather electropositive and it is bonded to this region (H in Vpd, Q_{R2} = 0.186 au). In the case where R_2 is electronegative (see data associated with Q_{CR2} in Etvpd, Etavpd, and Dmvpd), it also induces an asymmetric electronic distribution, and consequently, the C_8═O_9 bond is very polar (i.e., relatively high values of $|Q_{O9}|$ and $|Q_{C8}|$ are predicted).

(ii) Q_{C8} is relatively high if R_2 is electronegative (Q_{CR2} is very negative or less positive, Dmvdp/Suvpd), and it decreases appreciably with the increase of the electron-donor character of R_2 (Q_{CR2} very positive, Vdp).

When considering the polarity of the C_8—N_{10} bond and the electronic effects of R_2 from the analysis of data presented in Table 3, we can recognize the following behavior: $|Q_{N10}|$ decreases, and $n_{N10} \rightarrow \pi^*_{C=O}$ increases with the increase of the R_2 electron-attractive character. However, we deem it important to point out some exceptions to this rule when considering the variation of Q_{CR2} with Q_{N10} in Etavpd or when considering the change in the two values associated with Q_{CR2} and $n_{N10} \rightarrow \pi^*_{C=O}$ of Dmvpd and Chvpd versus that assigned to Etvpd and/or Ipvpd. In this regard, we see that relatively high values of $|Q_{N10}|$ and $n_{N10} \rightarrow \pi^*_{C=O}$ in Etavpd and Chvpd cannot be associated to the fact that the acyl substituent has a rather low electronegativity.

We deem that it is sensible to assume that the abnormalities pointed out before probably are a consequence of the existence of hyperconjugative effects acting in such a way to delocalize the electronic charge in N_{10} and R_2. From this point of view, we could understand that in these structures, the delocalization of lp_{N10} in R_2 via hyperconjugative effects is limited because the

Scheme 1. Local Interactions of Side Chains with the Polar O9═C8—X10 Backbone[a]

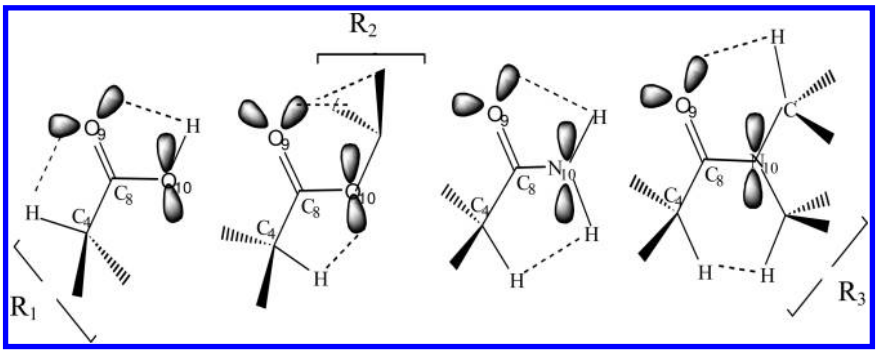

[a] Numbering scheme common for all of the derivatives in O9═C8—X10.

orbitals associated with acyl groups are rather poor electron acceptors [—$(CH_2)_2$—NH_2 in Etavpd) or they locate in an unfavorable spatial conformation to interact with lp_{N10} [—(C_6H_{12}) in Chvpd].

Regarding the relatively low values of $|Q_{N10}|$ and $n_{N10} \rightarrow \pi^*_{C=O}$ in Dmvpd, we assume that in —CH_3, the orbitals are good electron acceptors, and they localized in such a way to have a very effective charge stabilization of the N_{10} electronic charge and lp_{N10} in the acyl region but not over the π system.

From the foregoing discussion, we consider that the structural changes in the polar group of Vpa and it derivatives cannot be interpreted as a result of electronic effects of O_9 in C_8═O_9, from the electrostatic effects of $C_8^{\delta+}$, and of the stabilization of the n_{X10} from the $n_{X10} \rightarrow \pi^*_{C=O}$. From this evidence, we concluded that in Vpa and its derivatives, there are local interactions between the side chains and the polar backbone (Scheme 1) which could be responsible for the structural and electronic properties summarized in Tables 2 and 3. In fact, it is possible to think that in Vpa and it derivatives, there are stabilizing interactions between some C—H bonds of R_1 and R_2 groups and the polar moiety which act not only to induce structural changes on the C_8═O_9 and C_8—X_{10} bonds and part of the R_1 and R_2 groups but also to regulate the polarization of the π-system

C. Conformational Properties of the R_1 and R_2 Bonds Adjacent to the O_9═C_8—X_{10} Moiety. With the aim to explore the electron delocalization from the polar moiety to the different substituents, we examine the structural characteristics of the molecular $[(O/N/C—H)_{R2}\cdots O_9]$, $[(C—H)_{R2}\cdots O_{10}]$, $[(C_4—H)_{R1}\cdots H—N_{10}/O_{10}]$, and $[(C_4—H)_{R1}\cdots(H—C)_{R2}]$ subspaces, focusing on the distance values $r_{H\cdots O}$ and $r_{H\cdots H}$ and the improper angles $\alpha_{C8=O9\cdots(H)R2}$, $\alpha_{(O/N/C—H)R2\cdots O9}$, $\alpha_{C8—O10\cdots(H)R1}$, $\alpha_{(C4—H)R1\cdots O10}$, $\alpha_{N10—H\cdots(H)R1}$, $\alpha_{(C4—H)R1\cdots(H)R2}$, $\delta_{C8=O9\cdots(H—C/N/O)R2}$, $\delta_{C8—O10\cdots(H—C4)R1}$, $\delta_{N10—H\cdots(H—C4)R1}$, and $\delta_{(C4—H)R1\cdots(H—C/N)R2}$ (see Table 4).

As shown in Table 4, between O_9, X_{10}, N_{10}—H bonds and the neighboring C/O—H bonds, there are distances shorter than the conventional sum of the van der Waals radii ($r_{H\cdots H} < \sum r(vdW)[H,H] = 2.4$Å and $r_{H\cdots O} < \sum r(vdW)[H,O] = 2.72$Å) in a three-dimensional array with a very bent plane angle ($55.6° < \alpha_{N10—H\cdots H}$, $\alpha_{C—H\cdots H}$, $\alpha_{CH\cdots O10}$, $\alpha_{C8=O9\cdots H} \geq 124.5°$) and values of improper dihedral angles that are nearly planar ($-28.5° \leq [\delta_{(X10/C—H)R2\cdots O9=C8}$ and $\delta_{(C—H)R1\cdots H—N10}] \leq 36.5°$ in Vpa and amides; $-1.1° \leq [\delta_{(C—H)R2\cdots O10—C8}] \leq 12.9°$ and $-53.3° \leq [\delta_{C—H\cdots O9=C8}] \leq 50.1°$ in esters). We interpret that these data reveal a very soft repulsion potential in the considered molecular subspaces, and it indicates the existence of an important electric field acting on the H···O and H···H atoms in Vpa and the corresponding derivatives.

From the all of the data, we interpret that the bending away from coplanarity of the atoms in the polar moiety is accompanied by a three-dimensional arrangement of donor and acceptor proton units closing nearly planar pseudorings of four, five, and six members aligned at sufficiently short distances (2.122 Å $\leq r_{H\cdots O} \leq$ 2.668Å) to allow stabilizing interactions around the O_9═C_8—X_{10} backbone.

An aspect that it is worth mentioning from Table 4 is the fact that independent of the replacement of —OH by the esters or the presence (or absence in Dmvpd) of the N—H group in amides, there is no evidence of important structural changes within the pseudorings around the polar moiety. Beyond the low basicity of the ester group compared to the amide one, in all of the molecules, we detected very short interatomic distances between the O_9═C_8—X_{10} fragment and the adjacent R_1 and R_2 moieties. We understand that the slight structural differences predicted on $[(C_4—H)_{R1}\cdots H—N_{10}/O_{10}]$ reflect the presence or absence of a given functional group and the size. In fact, the presence of a N_{10}—H bond, a few more larger and with an electron density more concentrated between the nucleus than the lone pairs over O_{10}, explains why in amides, the $r_{H\cdots H}$ are shorter and the pseudorings are less bent (see structural parameters in $N_{10}—H\cdots(H—C)_{R1}$ against $(C_4—H)_{R1}\cdots O_{10}$). In other words, it is possible to indicate that independent of the atomic constitution of the O_9═C_8—X_{10} unit (where X_{10} = O or N) and of the type and size of the substituent, the fact that the planarity of the polar region is not appreciably disturbed with the change H $\rightarrow$ R_2 is consequence also of the establishment of intramolecular interactions between the O_9, O_{10}, and N_{10}—H bonds and the neighboring X_{10}/O/C—H bonds.

D. Topological ELF Analysis. With the aim to study the electronic delocalization around the polar region in the Vpa and its derivatives, we begin exploring the electronic properties of the bonds in the polar region obtained from ELF calculations. On the basis of the interpretation given by Silvi and Savin,[33,34] in Table 2S (Supporting Information), we summarized data on the ELF topology of the polar group in terms of the populations ($\overline{N}$) of the valence disynaptic attractors (basins) $V(C_4,H)$, $V(C_8,C_4)$, $V(C_8,O_9)$, $V(C_8,X_{10})$, and $V(H,X_{10})$, describing the C_4—H, C_4—C_8, C_8═O_9, C_8—X_{10}, and X_{10}—H bonds and the $V(O_9)$,$V(X_{10})$ monosynaptic valence attractors, representing the electron lone pairs of the O_9 and X_{10} atoms in C_8═O_9 and C_8—X_{10} bonds (Scheme 2).

Data in Table 2S (Supporting Information) show for Vpa and its derivatives, bonds C_4—H and C_4—C_8 with a clear covalent

Table 4. (A) Three-Dimensional Configuration of Intramolecular Distances $(C—H)_{R2}\cdots O_9$, $N_{10}—H\cdots(H—C_4)_{R1}$, and $(C—H)_{R2}\cdots(H—C_4)_{R1}$ in Amides of Vpa and (B) Three-Dimensional Configuration of Intramolecular Distances $(C—H)_{R2}\cdots O_9$ and $(C_4—H)_{R1}\cdots O_{10}$ in Esters and Vpa at B3LYP/6-311++G (6d,10f)[a]**

(A) contacts	Aphvpd	Suvpd	Bzvpd	Etvpd	Etavpd	Dmvpd	Chvpd	Ivpd	Vpd
				$(C—H)_{R2}\cdots O_9$					
$r_{H\cdots O}$	2.518	2.205	2.315	2.386	2.39	2.228	2.465	2.464	2.496
$r_{C\cdots O}$	2.819	2.894	2.835	2.824	2.845	2.718	2.829	2.834	2.267
$\alpha_{(C—H)s\cdots O}$	94.2	119.5	106.9	102.1	103.1	104.8	97.8	98.1	65.2
$\alpha_{C=O\cdots H}$	79.8	104.7	82.9	82.2	82.3	86.6	80.5	80.9	54.6
$\delta_{C—H\cdots O=C}$	36.5	4.8	5.02	18.5	13.7	−4.6	30.9	−28.5	−0.6
				$N_{10}—H\cdots(H—C_4)_{R1}$					
$r_{H\cdots H}$	2.174	2.093	2.156	2.167	2.149		2.155	2.166	2.245
	—	2.26	—	—	—		—	—	—
$r_{N\cdots C}$	2.463	2.459	2.456	2.461	2.462		2.462	2.463	2.459
$\alpha_{N—H\cdots H}$	96.9	101.1	96.8	97.6	98.2		98.05	97.5	93.2
	—	98.5	—	—	—		—	—	—
$\alpha_{C—H\cdots H}$	98.6	98.9	97.9	98.2	98.5		98.6	98.5	97.9
	—	89.5	—	—	—		—	—	—
$\delta_{C—H\cdots H—N}$	−3.014	1.1	19.4	3.9	−6.5		−0.55	−2.5	−7.8
				$(C—H)_{R2}\cdots(H—C_4)_{R1}$					
$r_{C—H}$						1.086			
$r_{H\cdots H}$	—		—	—	—	1.839	—	—	—
$r_{C\cdots C}$	—		—		—	3.054			
$\alpha_{(C—H)v\cdots H}$	—		—	—	—	124.1	—	—	—
$\alpha_{(C—H)s\cdots H}$	—		—	—	—	123.6	—	—	—
$\delta_{C—H\cdots H—C}$	—		—	—	—	−3.2	—	—	—

(B) contacts	Benvpa	Ispvpa	Secvpa	Prvpa	Isbvpa	Vpa
			$(C—H)_{R2}\cdots O_9$			
$r_{H\cdots O9}$[b]	2.62	2.628	2.016	2.622	2.122	2.281
	2.62	2.634	2.557	2.645	2.603	—
$r_{C\cdots O9}$	2.672	2.681	2.777	2.681	2.672	—
$\alpha_{(C—)s\cdots O9}$	80.8	80.8	127.3	81.1	122.9	75.8
	80.8	80.6	110.9	80	81.7	—
$\alpha_{C8=O9\cdots H}$	77.6	77.4	99.1	77.7	98.2	55.8
	77.6	77.2	92.2	76.9	76.6	—
$\delta_{C—H\cdots O9=C8}$	49.8	−49.1	6.8	−50.6	18.9	0
	−49.8	49.8	−35.6	48.5	−53.3	—
			$(C_4—H)_{R1}\cdots O_{10}$			
$r_{H\cdots O10}$	2.375	2.379	2.382	2.394	2.392	2.511
$\alpha_{C—H\cdots O10}$	77.4	77.2	76.9	76.1	76.6	73.4
$r_{C\cdots O10}$	2.388	2.389	2.387	2.383	2.431	2.437
$\alpha_{C—O10\cdots H}$	62.8	62.7	62.6	61.9	61.9	55.9
$\delta_{C4—H\cdots O10—C}$	−0.01	−1.1	−3.756	12.9	9.9	0

[a] Subscript R1 indicates a C—H bond in the valproyl moiety; subscript R2 indicates C—H bonds of the acyl substituent. Distances are in Å, and angles are in degrees. [b] Data are the geometrics of bifurcated contacts between the neighboring C—H bonds of the acyl substituent and the O carbonylic.

character ($2.03 \leq \overline{N} \leq 2.20$ e). Regarding the different populations between the V(C4,H) and V(C4,C8) basins and its change with the structural modification of their environment, we understand that they are a direct consequence of its position with respect to the polar regions and the variation of the electronic effects acting on them. The basins of the greatest $\overline{N}$ will be that closer to the $O_9{=}C_8—X_{10}$ moiety and with the $O_9{=}C_8—X_{10}—R_2$ group most electron-withdrawing.

From the multivariate analysis, ELF values of fluctuation σ^2 and λ for the basins in $O_9{=}C_8—X_{10}$ reveal the degree of delocalization of the electronic density between adjacent basins.[35] Then, for Vpa and its derivatives, values of $0.66 \leq \sigma^2 \leq 1.56$ and $0.33 \leq \lambda \leq 0.79$

dx.doi.org/10.1021/jp1081998 |J. Phys. Chem. A 2011, 115, 1686–1700

Scheme 2. Numbering and Topology ELF of the Polar Region and Atoms Adjacent to Vpa, Vpd, and Secvpa[a]

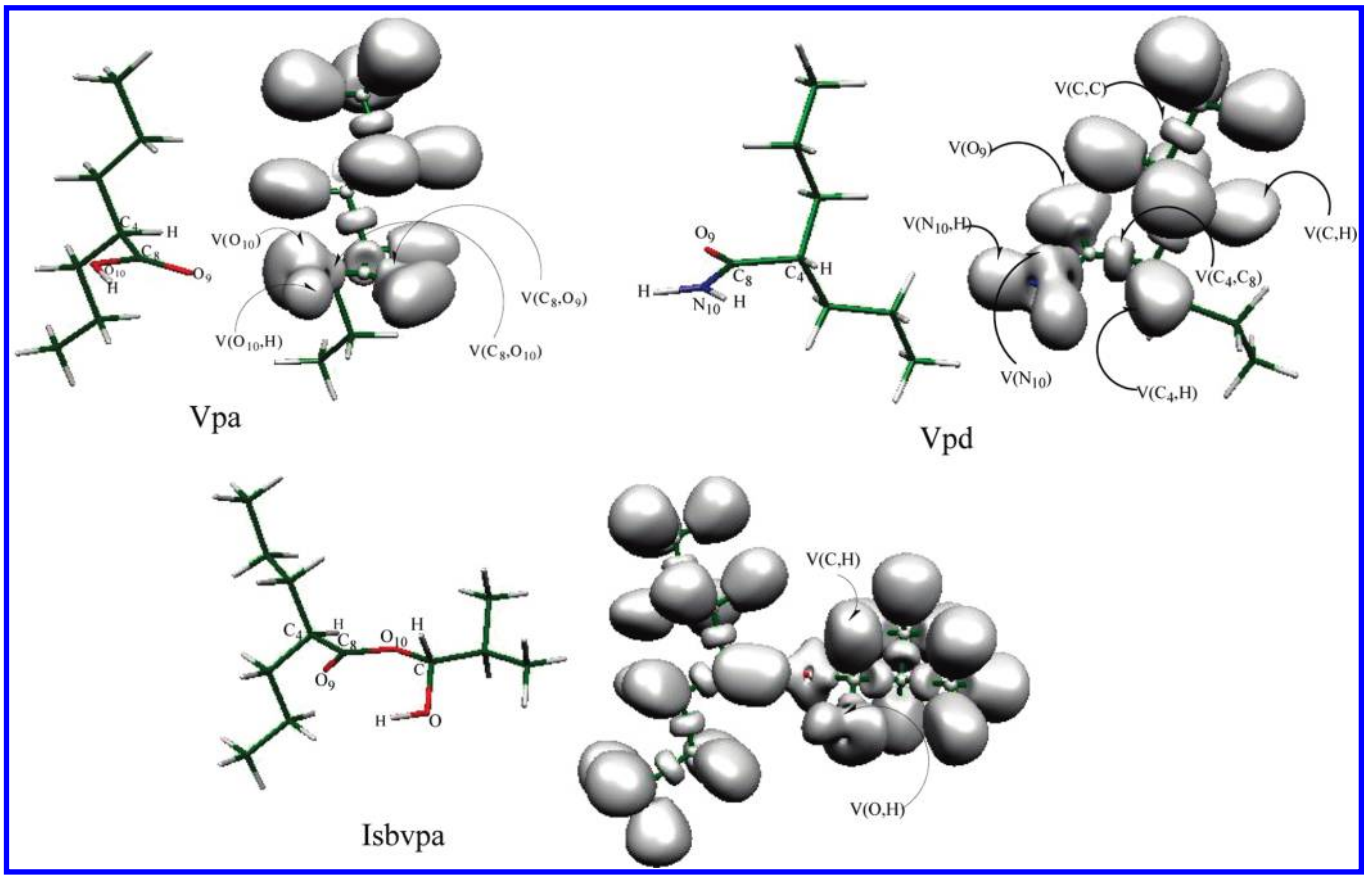

[a] The numbering in O═C—O/N is common in all molecules and is in accord with the numbering scheme in Figure 1 for Vpa. The neighboring atoms of substituents linked to the polar moiety are C, O, and H.

indicate that in this region, the atoms form polar covalent bonds, and the electrons are highly delocalized.

Regarding the bonds in the O_9═C_8—X_{10} unit, they present an electronic population intermediate between a simple and a double bond [2.19 ≤ V(C_8,O_9) ≤ 2.45 e and 1.63 ≤ V(C_8, X_{10}) ≤ 3.08 e], and the V(X_{10},H) basin has a population of almost 2 e [1.76−2.01 e]. In relation to the basins describing the lone electron pairs of O_9 and X_{10} (populations of the V(O_9) and V(X_{10}) domains), Table 2-S (Supporting Information) reveals the existence of subspaces with an electron density ranging from 5.31 (Vpa) to 5.55 e (Chvpd) for V(O_9); for the V(O_{10}) basins, the electron population values increase in the range of 4.33 (Vpa)−4.42 e (Benvpa, Isbvpa), while for the V(N_{10}) basins, the population is predicted to be in the range of 0.92 (Chvpd)−1.78 e (Vpd).

To investigate the delocalization of the electron density of the O_9═C_8—X_{10} moiety in vicinal V(C,C/H) domains, we analyze the covariance matrix whose elements designed as cov[Ω_i,Ω_j] reveal the correlation between the electron density distribution in basins Ω_i and Ω_j.[35] Values of cov[V(O_9),V(C,H)$_{R1,R2}$], cov[V(X_{10}),V(C,H/C)$_{R2}$], cov[V(O_{10})/V(N_{10},H)/V(C,H)$_{R2}$, and V(C_4,H)] are collected in Table 5.

We interpret that each value in Table 5 indicates the existence of electrostatic interactions between atoms of different electronegativities with a transference charge ranging from 0.01 to 0.16 e around the O_9═C_8—X_{10} moiety. The delocalization V(C_4,H) ↔ V(N_{10},H)/V(C,H) in amides is noteworthy. According to our calculation, values of transferred charge of 0.02 and 0.04 e suggest the existence of stabilizing interactions between pairs of hydrogen atoms bearing similar electrical charge.

According to this evidence, we recognize that around the O_9═C_8—X_{10} backbone in Vpa and its derivatives, there is electronic delocalization of the lone pair orbital of the O_9 and X_{10} atoms and the N_{10}—H bond within of the vicinal (—CH/C)$_{R1,R2}$ bonds.

Searching for more evidence on the electronic delocalization around the polar region of the structure under study, all possible interactions between "filled" (electron donor) Lewis-type NBOs and "empty" (electron-acceptor) non-Lewis NBOs in the O_9═C_8—X_{10}, R_1, and R_2 moieties and their energetic importance are examined in the following.

E. NBO/ELF Analysis. In the NBO language, the donor−acceptor interaction type $n_B \rightarrow \sigma^*_{A—H}$ or $\sigma_{C—H} \rightarrow \sigma^*_{A—H}$ entails a delocalization of the electron density from the lone pair (n_B) of the Lewis base B or a $\sigma_{C—H}$ hydride bonding orbital into the unfilled $\sigma^*_{A—H}$ hydride antibonding orbital of the Lewis acid (AH). The net electronic effect due to the partial transferred charge is a n_B or $\sigma_{C—H}$ with a partial positive charge and a $\sigma^*_{A—H}$ with a partial negative charge.

The charge transferred in a general donor−acceptor interaction can be approximated as $Q_{i\rightarrow j^*} = 2(\langle\phi_i|\hat{F}|\phi_j^*\rangle^2/(\varepsilon_j^* - \varepsilon_i)^2)$,[36] where ϕ_i and ϕ_j^* are the donor and acceptor orbitals, ε_j^* and ε_i are the energies of the orbitals under consideration, and $\hat{F}$ is the Fock operator.

Table 5. Covariance Values, cov[Ω_i,Ω_j], Representing the Correlation between the Basin Population Calculated for the $V(O_9)$, $V(X_{10})$, $V(N_{10},H)$, $V(C,H)_{R2}$, $V(C,H)_{R1}$, and $V(C,H/C)_{R2}$ Basins, that is, $V(O_9) \leftrightarrow V(C,H/C)_{R1,R2}$, $V(X_{10}) \leftrightarrow V(C,H/C)_{R2}$, $V(O_{10}) \leftrightarrow V(C_4,H)$, $V(C_4,H) \leftrightarrow V(N_{10},H)$, and $V(C_4,H) \leftrightarrow V(C,H)_{R2}$[a]

	cov[Ω_i,Ω_j]		
molecules	[$V(O_9)$, $V(C,H/C)_{R1,R2}$]	[$V(X_{10})$,$V(C,H/C)_{R2}$]	[$V(O_{10})$/ $V(N_{10},H)/V(C,H)_{R2}$, $V(C_4,H)$]
Benvpa	0.03	0.16	0.02
Ispvpa	0.04	0.16	0.02
Secvpa	0.06	0.16	0.02
Prvpa	0.05	0.16	0.02
Isbvpa	0.08	0.19	0.02
Vpa	0.03		
Aphvpd	0.05	0.08	0.02
Suvpd	0.08	0.04	0.02
Bzvpd	0.04	0.07	0.02
Etvpd	0.05	0.05	0.02
Etavpd	0.04	0.07	0.02
Dmvpd	0.07	0.20	0.04
Chvpd	0.04	0.11	0.02
Ipvpd	0.06	0.05	0.02
Vpd	0.03		0.01

[a] Subscript R_1 indicates the C—H bond in the valproyl moiety, and subscript R_2 indicates C—H bonds of the acyl substituent.

In Table 3-S (Supporting Information), we present the tabulation of the different donor−acceptor interactions found in Vpa and its derivatives around the $O_9{=}C_8{-}X_{10}$ backbone.

According to our data in Table 3-S (Supporting Information), the alignment of the C—H/C bonds in the vicinity of the $O_9{=}C_8{-}X_{10}$ moiety in some derivatives is a consequence of electrostatic interaction types: $n_{O9} \rightarrow \sigma^*_{C/O-H}$ as it is indicated for Secvpa, Isbvpa, Suvpd, Bzvpd, and Dmvpd; $n_{O9} \rightarrow \sigma^*_{C-C}$ as it is indicated for Benvpa, Ispvpa, Prvpa, and Dmvpd; and $n_{O9} \rightarrow \sigma^*_{C-C}$ and $\sigma^*_{C-C} \rightarrow \sigma^*_{O-H}$ in Isbvpa.

In all esters and amides, we also recognized in $[(C{-}H/C)_{R2}\cdots O_9]$ a transference of charge via the electrostatic interactions: $n_{O9} \rightarrow \sigma^*_{C4-C8}$ and $\sigma_{C4-C8} \rightarrow \sigma^*_{X10-H/C}$ and $n_{O9} \rightarrow \sigma^*_{C4-C8}$, $\sigma_{C4-C8} \rightarrow Ry^*_{N10}$, $n_{N10} \rightarrow \sigma^*_{C-H}/n_{N10} \rightarrow \sigma^*_{C-C}$, or $n_{O9} \rightarrow Ry^*_{C/H}$ (the transferred charge comes to a virtual orbital of C or H, $Ry^*_{C/H}$)

Similarly, in the $[(C_4{-}H)_{R1}\cdots O_{10}]$ region of the esters, we recognized the delocalization paths $n_{O10} \rightarrow \sigma^*_{C8=O9}$ and $\sigma_{C8=O9} \rightarrow Ry^*_{C4}$, and in the $[(C_4{-}H)_{R1}\cdots H{-}N_{10}/C]$ subspace in amides, the delocalization occurs through the donor−acceptor interactions: $\sigma_{C4-H} \rightarrow \sigma^*_{C8=O9}$, $\sigma_{C8=O9} \rightarrow \sigma^*_{N-H}$, and $\sigma_{C4-H} \rightarrow \sigma^*_{C-H}$ only in the tertiary Dmvpd amide.

We interpret that these results show that in Vpa and its derivatives, there are very flexible functional groups such as X_{10}—H, C—H, and C—C which participate in attractive interactions with moieties such as $C_8{=}O_9$, $-\ddot{O}{:}_{10}$, $-\ddot{N}_{10}$, and $C_4{-}H$ in a nearly coplanar arrangement with atoms such as C_8, O_9, X_{10}, and $C_{R1/R2}$ at $r_{C\cdots N}$, $r_{C\cdots O}$, $r_{H\cdots O}$, and $r_{C\cdots C}$ distances shorter than the sum of their van der Waals radii.

From NBO data, it can be seen also that in the $[(O/N/C{-}H)_{R1,R2}\cdots O_9]$, $[(C{-}H)_{R2}\cdots O_{10}]$, $[(C_4{-}H)_{R1}\cdots H{-}N_{10}/O_{10}]$, and $[(C_4{-}H)_{R1}\cdots(H{-}C)_{R2}]$ intramolecular regions,

Table 6. Exchanged NBO Charge in the $[(O/N/C{-}H)_{R1,R2}\cdots O_9]$, $[(C{-}H)_{R2}\cdots O_{10}]$, $[(C_4{-}H)_{R1}\cdots H{-}N_{10}/O_{10}]$, and $[(C_4{-}H)_{R1}\cdots(H{-}C)_{R2}]$ Regions Considering Only the Transferred Charge through the TSI Mechanism and the Charge That Arrives to the Final Electron-Acceptor Orbital in the TBI Path[a]

molecules	$\sum n_{O9} \rightarrow (\sigma^*_{C-H/C})_{R1,R2}$	$\sum n_{X10} \rightarrow (\sigma^*_{C-H/C})_{R2}$	$n_{O10},\sigma_{N10-H} \rightarrow (\sigma^*_{C-H})_{R1}$
Benvpa	0.0094	0.0281	0.0006
Isvpa	0.0091	0.0304	0.0006
Secvpa	0.0167	0.0375	0.0006
Prvpa	0.0092	0.0300	0.0005
Isbvpa	0.013	0.0374	0.0005
Vpa	0.0046	0.0026	0
Aphvpd	0.0072	0.0329	0.0015
Suvpd	0.0107	0.2089	0.0014
Bzvpd	0.0087	0.0372	0.0014
Evpd	0.0072	0.0356	0.0015
Etavpd	0.0072	0.0335	0.0015
Dmvpd	0.011	0.0712	0.0019
Chvpd	0.0071	0.0325	0.0015
Ipvpd	0.0067	0.0349	0.0015
Vpd	0.0045	0.0008	0.0013

[a] The values are in au.

there are two kinds of charge transference mechanisms. Data in Table 3-S (Supporting Information) suggest that while in Secvpa, Isbvpa, Suvpd, Bzvpd, and Dmvpd there exists a direct overlap of the n_{O9} and σ^*_{CH} orbitals in the $(H{-}C)_{R2}\cdots O_9$ path (through space interactions, TSI), for the other molecules, an indirect overlap between them through the chain of chemical bonds that they connect (through bond interactions, TBI) was found.[36,37] Likewise for Benvpa, Ispvpa, Prvpa, and Dmvpd, we have found that n_{O9} is delocalized within the σ^*_{C-C} orbital via a TSI mechanism.

On the other hand, while in the esters the $n_{O10} \rightarrow \sigma^*_{C8=O9}$ and $\sigma_{C8=O9} \rightarrow Ry^*_{C4}$ donor−acceptor interactions and the paths $\sigma_{C4-H} \rightarrow \sigma^*_{C8=O9}$ and $\sigma_{C8=O9} \rightarrow \sigma^*_{N-H}$ in the primary and secondary amides indicate an indirect overlap between the $n_{O10}/C_4{-}H$ and $C_4{-}H/H{-}N_{10}$ moieties (TBI mechanism), for Dmvpd, an interaction via TSI ($\sigma_{C-H} \rightarrow \sigma^*_{C4-H}$) in the $C_4{-}H\cdots H{-}C$ region is predicted.

With the aim to compare how ELF and NBO data describe the charge delocalization around the $O_9{=}C_8{-}X_{10}$ group, we evaluate the degree of correlation of the sum of cov[$V(O_9)$,$V(C,H/C)_{R1,R2}$] and cov[$V(X_{10})$,$V(C,H/C)$], that is, $\sum$ cov[$V(O_9)/V(X_{10})$,$V(C,H/C)_{R1,R2}$], along with the sum of the exchanged NBO charge in the $[(O/N/C{-}H)_{R1,R2}\cdots O_9/X_{10}]$ regions, considering only the transferred charge through the TSI mechanism and the charge that arrives at the final electron acceptor orbital in the TBI path ($\sum\sum n_{O9}/n_{X10} \rightarrow \sigma^*_{C-H}/\sigma^*_{C-C}/Ry^*_{C/H}$) (Table 6).

We did not consider the charge of the intermediate donor−acceptor interactions in the TBI mechanism because there is not a quantitative agreement between ELF charges and the total delocalized charge in a TBI mechanism. We deem that the last effect is due to the fact that not all of the exchanged charge in the TBI path arrives at the final acceptor orbital.

In addition,because the exchanged ELF and NBO charges in the $[(C_4{-}H)_{R1}\cdots H{-}N_{10}/O_{10}]/[(C_4{-}H)_{R1}\cdots(H{-}C)_{R2}]$ regions (values of cov[$V(O_{10})$,$V(C_4,H)$]/cov[$V(C_4,H)$,$V(N_{10},H)$]

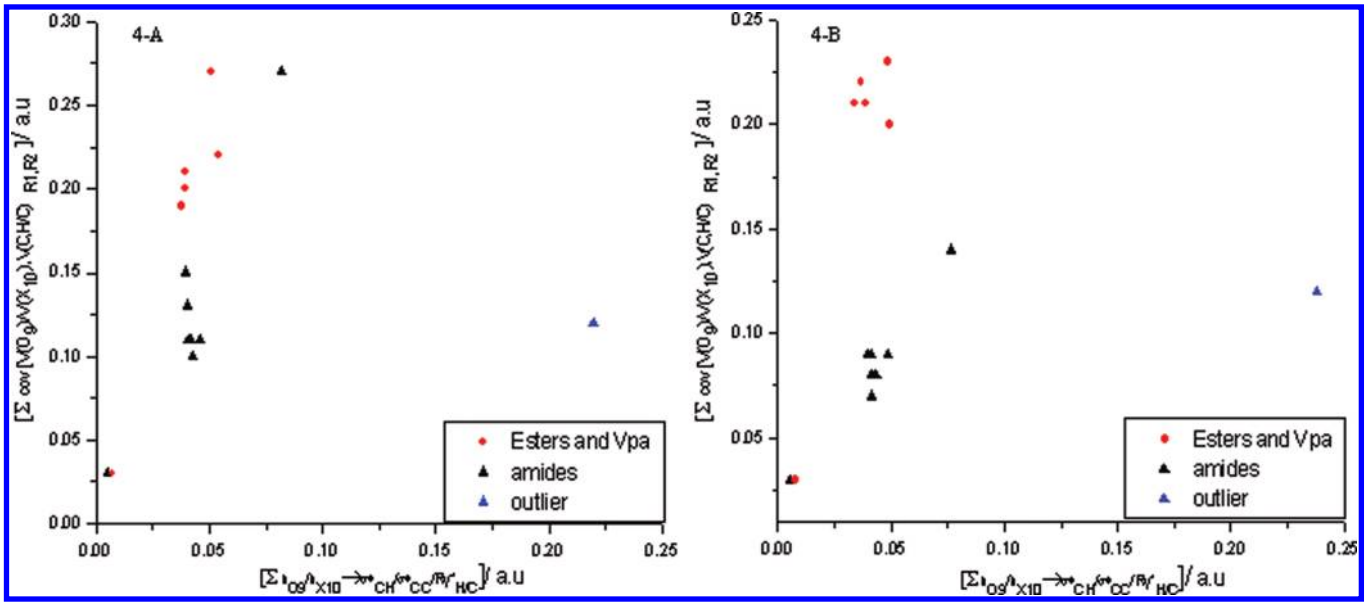

Figure 4. Relationship between the $\sum$ cov[V(O_9)/V(X_{10}),V(C,H/C)$_{R1,R2}$] ELF and $\sum n_{O9}/n_{X10} \rightarrow \sigma^*_{C—H}/\sigma^*_{C—C}/Ry^*_{C/H}$ NBO charge.

and NBO charge $\sigma_{C8=O9} \rightarrow Ry^*_{C4}/\sigma_{C8=O9} \rightarrow \sigma^*_{N—H}$) do not show significant variations along the series of derivatives, we do not evaluate the relationship between these values (see Tables 5 and 3-S (Supporting Information)).

In Figure 4, we plotted the relationship values of $\sum$ cov-[V(O_9)/V(X_{10}),V(C,H/C)$_{R1,R2}$] against $\sum n_{O9}/n_{X10} \rightarrow \sigma^*_{C—H}/\sigma^*_{C—C}/Ry^*_{C/H}$. The scatter plot indicates the existence of linear relationships between the variables considered, and therefore, the linear correlation coefficient of the Pearson (R) parameter was analyzed. Excluding the outlier value (point numerically distant from the rest of the data, Suvpd), the good linear correlation between $\sum$ cov[V(O_9)/V(X_{10}),V(C,H/C)$_{R1,R2}$] and $\sum n_{O9}/n_{X10} \rightarrow \sigma^*_{C—H}/\sigma^*_{C—C}/Ry^*_{C/H}$ (Pearson correlation coefficient, R = 0.95) shows the agreement between the description of the charge delocalization around O_9═C_8—X_{10} obtained through the ELF and the NBO methods.

Beyond the predicted quantitative differences and in the context of linking molecular properties obtained from different conceptual approaches, we interpret that the covariance values in the [$(C_4—H)_{R1}\cdots H—N_{10}/O_{10}$]/ [$(C_4—H)_{R1}\cdots(H—C)_{R2}$] regions correlate with the NBO charge and that the abnormalities observed (the disparities between ELF and NBO trends in the outlier, the greatest differences against the values of $\sum\sum$ cov [V(O_9)/V(X_{10}),V(C,H/C)$_{R1,R2}$] in amides and esters with respect to that indicated for $\sum n_{O9}/n_{X10} \rightarrow \sigma^*_{C—H}/\sigma^*_{C—C}/Ry^*_{C/H}$ or slight differences of the NBO charges for the same value of $\sum$ cov[V(O_9)/V(X_{10}),V(C,H/C)$_{R1,R2}$]; see Figure 4) are a consequence of the methodological differences between both formalisms. In fact, while the NBO charge is highly sensitive to stereoelectronic factors that regulate the hyperconjugative interactions,[36,38] ELF data mask such information.

F. Atoms in Molecules Analysis. From the data on structural and electronic features, we now advance in our theoretical analysis, resorting to the quantum theory of AIM to classify the stabilizing interactions around the polar moiety in Vpa and its derivatives due to the well-known ability of this methodology to provide conclusive answers to the question of whether two atoms are linked or not.[39] From the concept that indicates that two atoms are bonded if their nuclei are linked through the space by a line of maximum electron density called bond path, the search for critical points in the molecular [$(O/N/C—H)_{R2}\cdots O_9$], [$(C—H)_{R2}\cdots X_{10}$], [$(C_4—H)_{R1}\cdots H—N_{10}/O_{10}$] and [$(C_4—H)_{R1}\cdots(H—C)_{R2}$] subspaces only indicates points where the gradient of the electron density vanishes [$\nabla\rho(r_c) = 0$] for the $(O—H)_{R2}\cdots O_9$ region in Secvpa and Isbvpa, for $(C—H)_{R2}\cdots O_9$ in Suvpd, and for $(C—H)_{R2}\cdots H—C_4$ in Dmvpd (see Table 7).

Table 7. Topological Properties of the Bond Critical Points Found in Secvpa, Suvpd, and Dmvpd within the Contacts C/O—H···O and C—H···H—C

	$(O—H)_{R2}\cdots O_9$		$(O—H)_{R2}\cdots O_9$	$(C—H)_{R2}\cdots(H—C_4)_{R1}$
properties	Secvpa	Isbvpa	Suvpd	Dmvpd
$\rho(r_c)$	0.025	0.02	0.019	0.017
$\nabla^2\rho(r_c)$	0.088	0.072	0.067	0.058
G_C	0.021	0.017	0.015	0.012
V_C	−0.019	−0.015	−0.012	−0.009
H_C	0.002	0.002	0.003	0.003

Topological parameters found for the bond critical points (Table 7) satisfy the criteria proposed by Koch and Popelier[40] to detect weak hydrogen bonding [$0.002 < \rho(r_c) < 0.040$ au and $0.024 < \nabla^2\rho(r_c) < 0.139$ au]. According to our calculation, these data clearly reveal the existence of weak H bonds characterized by a small value of $\rho(r_c)$, $\nabla^2\rho(r_c) > 0$, and a very small and positive electronic energy density H_C of the charge distribution. This last amount may be expressed as $H_c = G_C + V_C$,[18,40] where G_C is a local one-electron kinetic energy density and V_C is the local potential energy density.

It is noteworthy that the bond path predicted by AIM between two atoms of H in Dmvpd is a closed shell, stabilizing interaction that should be called a hydrogen—hydrogen bond according to Matta and co-worker.[41]

Exploring the structural features of the bridges where AIM identifies hydrogen bonds, it is worth highlighting that this methodology characterizes critical points on hexa-atomic pseudorings with $\alpha_{O9\cdots H—O}$, $\alpha_{O9\cdots H—C}$, and $\alpha_{H\cdots H—C}$ >100° (see Table 4),

dx.doi.org/10.1021/jp1081998 |J. Phys. Chem. A 2011, 115, 1686–1700

where electronic exchange occurs via a TSI mechanism. Then, we notice the difficulty of this methodology to identify bond paths in pseudorings of four and five atoms where improper interior angles are <100° and where the electronic exchange is via TBI.

From the foregoing discussion, we can assert that there are stabilizing electrostatic interactions around the $O_9{=}C_8{-}X_{10}$ unit, which, as it is well-known,[28,37] may influence the conformational equilibrium, modify the reactivity, and determine the molecular recognition speed and charge transfer of a functional group in chemical or biological processes that are initiated after the establishment of intermolecular interactions such as hydrogen bonds.

With the aim to analyze the relationship between these interactions and the electronic properties of the group $O_9{=}C_8{-}X_{10}$, we evaluate the correlation between the $n_{O9} \rightarrow \sigma^*_{C-H}/\sigma^*_{C-C}$ and $n_{X10} \rightarrow \sigma^*_{C-H}/\sigma^*_{C-C}/Ry^*_{C/H}$ transferred charges and the total transferred charge localized around the $O_9{=}C_8{-}X_{10}$ group ($\sum n_{O9/X10}/\sigma_{C4-H} \rightarrow \sigma^*_{C-H}/\sigma^*_{C-C}/Ry^*_{C/H}/\sigma^*_{N10-H}$) with the natural charge on the C_8, O_9, and X_{10} atoms.

G. Structure−Property Relationship. We carried out a statistical analysis of data considering separately the electronic properties of the moieties $O_9{=}C_8{-}O_{10}$ and $O_9{=}C_8{-}N_{10}$ due to the different electronic reorganization that an electroattractor or electrodonor R_2 induces on each one of these regions (see subsection B).

In Figure 1-S (Supporting Information), the graphic representation of the correlation between the variables Q_{O9}, Q_{C8}, and Q_{X10} and the charge values $n_{O9} \rightarrow \sigma^*_{C-H}/\sigma^*_{C-C}$, $n_{X10} \rightarrow \sigma^*_{C-H}/\sigma^*_{C-C}/Ry^*_{C/H}$, and $\sum n_{O9/X10}/\sigma_{C4-H} \rightarrow \sigma^*_{C-H}/\sigma^*_{C-C}/Ry^*_{C/H}/\sigma^*_{N10-H}$. We have evaluated the linear Pearson coefficient (R) because there is a scatter plot that indicates the existence of linear relationships between the variables considered.

As can be seen in Figure 1-S (Supporting Information), from the general trend of a negative linear correlation ($R < 0$) between the values Q_{O9} and $n_{O9} \rightarrow \sigma^*_{C-H}/\sigma^*_{C-C}$ and a positive linear relationship ($R > 0$) between the pairs of variables ($\sum n_{O9/X10}/\sigma_{C4-H} \rightarrow \sigma^*_{C-H}/\sigma^*_{C-C}/Ry^*_{C/H}/\sigma^*_{N10-H}$; Q_{C8}) and ($n_{X10} \rightarrow \sigma^*_{C-H}/\sigma^*_{C-C}/Ry^*_{C/H}$; Q_{X10}), we recognize that they explicitly reveal the cooperative effect of the donor−acceptor interactions in the delocalization of the π system of the $O_9{=}C_8{-}X_{10}$ group. Indeed, because the functional groups acting as an electron donor and acceptor are linked via a π system, we consider that the relationship between high electronic exchange in the intramolecular [$(O/N/C{-}H)_{R1,R2}\cdots O_9$], [$(C{-}H)_{R2}\cdots O_{10}$], [$(C_4{-}H)_{R1}\cdots H{-}N_{10}/O_{10}/C_{R2}$], and [$(C_4{-}H)_{R1}\cdots(H{-}C)_{R2}$] regions, high electronic population in O_9, and reduced negative charge on the C_8 and X_{10} atoms indicates an electronic charge redistribution in the group $O_9{=}C_8{-}X_{10}$ in such a way as to compensate for the charge that the electronegative atoms delocalize via donor−acceptor interactions $n_{O9} \rightarrow \sigma^*_{C-H}/\sigma^*_{C-C}$ and $n_{X10} \rightarrow \sigma^*_{C-H}/\sigma^*_{C-C}/Ry^*_{C/H}$.

According to the trends observed in Figure 1-S (Supporting Information), we interpret that the loss of negative charge on the electron-donor group is compensated for by the attraction of electrons of the polar region. In this way, it can be expected that together with the flow of electrons that counteracts the electronic effects induced by the interactions $n_{O9} \rightarrow \sigma^*_{C-H}/\sigma^*_{C-C}$ and $n_{X10} \rightarrow \sigma^*_{C-H}/\sigma^*_{C-C}/Ry^*_{C/H}$, the electronic changes in the regions adjacent to the electron-donor group (C_8, X_{10}) occur as predicted by the pair of variables $n_{X10} \rightarrow \sigma^*_{C-H}/\sigma^*_{C-C}/Ry^*_{C/H}$ (Q_{X10}) and $\sum n_{O9}/n_{X10} \rightarrow \sigma^*_{C-H}/\sigma^*_{C-C}/Ry^*_{C/H}$ (Q_{C8}).

On the other hand, on the basis of the relationships between the values of Q_{CR1} and Q_{CR2} with the total charge delocalized around the $O_9{=}C_8{-}X_{10}$ group (Figure 2-S, Supporting Information), a positive linear correlation between the variables $\sum n_{O9/X10}/\sigma_{C4-H} \rightarrow \sigma^*_{C-H}/\sigma^*_{C-C}/Ry^*_{C/H}/\sigma^*_{N10-H}$ and Q_{CR1} and a negative correlation between $\sum n_{O9/X10}/\sigma_{C4-H} \rightarrow \sigma^*_{C-H}/\sigma^*_{C-C}/Ry^*_{C/H}/\sigma^*_{N10-H}$ and Q_{CR2}, we interpret that they indicate that the partial positive charge on the electron-acceptor group does not diminish with the interactions $n_{O9} \rightarrow \sigma^*_{C-H}/\sigma^*_{C-C}$, $n_{X10} \rightarrow \sigma^*_{C-H}/\sigma^*_{C-C}/Ry^*_{C/H}$, $\sigma_{C4-H} \rightarrow \sigma^*_{N10-H}/\sigma_{C-H}$, and $n_{O10} \rightarrow \sigma^*_{C4-H}$. In fact, the relationship in the Figure 2-S (Supporting Information) reveals the electronic effect as a consequence of the compensatory mechanism that acts to delocalize the charge coming from the acceptor group on adjacent more electronegative nuclei; the decrease of negative charge on Q_{CR1} and the growth of the electronic population on Q_{CR2} with the increase of $\sum n_{O9/X10}/\sigma_{C4-H} \rightarrow \sigma^*_{C-H}/\sigma^*_{C-C}/Ry^*_{C/H}/\sigma^*_{N10-H}$ indicates that the charge that reaches the $\sigma^*_{C-H}/\sigma^*_{C-C}/Ry^*_{C/H}/\sigma^*_{N10-H}$ orbitals is transferred to adjacent nuclei, delivering electrons to the flow of charges that counteracts the loss of electrons from the most electronegative atoms due to the $n_{O9} \rightarrow \sigma^*_{C-H}/\sigma^*_{C-C}$ and $n_{X10} \rightarrow \sigma^*_{C-H}/\sigma^*_{C-C}/Ry^*_{C/H}$ exchanges.

Regarding the absolute value of the coefficient R (see Figures 1-S and 2-S, Supporting Information) as, in general, this is in the range of $|0.80-0.994|$, it is possible to infer from the percentage of determination coefficients (R^2)[42] that between 64.5 and 98.8% of the changes of the quantities Q_{O9}, Q_{C8}, Q_{X10}, Q_{CR1}, and Q_{CR2} can be explained from the values of $n_{O9} \rightarrow \sigma^*_{C-H}/\sigma^*_{C-C}$, $n_{X10} \rightarrow \sigma^*_{C-H}/\sigma^*_{C-C}/Ry^*_{C/H}$, and $\sum n_{O9/X10}/\sigma_{C4-H} \rightarrow \sigma^*_{C-H}/\sigma^*_{C-C}/Ry^*_{C/H}/\sigma^*_{N10-H}$.

Deviations from the behavior described above or observations numerically distant from the data set (outliers) were observed in structures where R_2 is an aryl ring (Aphvpd, Bzvpd, Suvpd). In these structures, a positive linear correlation between Q_{O9} and $n_{O9} \rightarrow \sigma^*_{C-H}/\sigma^*_{C-C}$ can be noted (R = 0.982; see Figure 1-S (Supporting Information)). We think that due to the proximity of the C_6H_5 moiety to the $O_9{=}C_8{-}X_{10}$ group, the polar region is part of a larger conjugated system involving the electron attractor group of R_2. In this case, besides the cooperative effects of delocalization of the π system, there are operating interactions through which the electron density of the polar region is delocalized over R_2.

The last statement arises from considering that the reason for the decrease of the electronic population on O_9 with the increase of $n_{O9} \rightarrow \sigma^*_{C-H}/\sigma^*_{C-C}$ is a consequence of the predominance of hyperconjugative effects that remove charge from the polar region in the structures Aphvpd, Bzvpd, and Suvpd over the compensatory cooperative mechanisms of polarization π-system or hyperconjugative effects that provide electron density to the electron-deficient center (C_8) in the polar region.

From this last remark, we deem that to perform a precise description of changes in structural and electronic properties of the $O_9{=}C_8{-}X_{10}$ group, it is not enough to consider the combined effects across space and through bonds identified in the intramolecular regions [$(O/N/C{-}H)_{R1,R2}\cdots O_9$], [$(C{-}H)_{R2}\cdots O_{10}$], [$(C_4{-}H)_{R1}\cdots H{-}N_{10}/O_{10}/C_{R2}$], and [$(C_4{-}H)_{R1}\cdots(H{-}C)_{R2}$] (Table 3-S, Supporting Information). In addition to these interactions, the intrinsic ability of R_1 and R_2 to disrupt the resonance of the $O_9{=}C_8{-}X_{10}$ group causing a net electronic displacement contrary to that dictated by the cooperative effects of delocalization of the π system and to analyze the change of the inductive and conjugative effects of R_1 and R_2 in the presence of a polar solvent should be assessed.

After analyzing the factors that control the charge distribution in the group $O_9{=}C_8{-}f_{10}$, we built a correlation matrix between

Table 8. Correlation Matrix between the Explanatory Variables of the Natural Charge of the Atoms in the Region O_9═C_8—X_{10} of Vpa and Its Derivatives ($n_{O9} \rightarrow \sigma^*_{C-H}/\sigma^*_{C-C}$, $n_{X10} \rightarrow \sigma^*_{C-H}/\sigma^*_{C-C}/Ry^*_{C/H}$, $\sum n_{O9/X10}/\sigma_{C4-H} \rightarrow \sigma^*_{C-H}/\sigma^*_{C-C}/Ry^*_{C/H}/\sigma^*_{N10-H}$, and $\sum^{O9=C8-O10}$) and the Structural Parameters τ, χ_{C8}, χ_{X10}, r_{C8-X10}, and $r_{C8=O9}$ in (A) Vpa and Its Derivatives with the Group O_9═C_8—O_{10} and (B) Vpd and Its Analogues

(A)

	$\sum n_{O9} \rightarrow (\sigma^*_{C-H/C})_{R1,R2}$	$\sum n_{X10} \rightarrow (\sigma^*_{C-H/C}/Ry^*_{C/H})_{R1,R2}$	$\sum^{O9=C8-O10}$	τ	χ_{C8}	χ_{O10}	r_{C8-O10}	$r_{C8=O9}$
$\sum n_{O9} \rightarrow (\sigma^*_{C-H/C})_{R1,R2}$	1							
$\sum n_{X10} \rightarrow (\sigma^*_{C-H/C}/Ry^*_{C/H})_{R1,R2}$	0.85	1						
$\sum^{O9=C8-O10}$	0.91	0.99	1					
τ	−0.52	−0.8	−0.76	1				
χ_{C8}	0.47	0.55	0.55	−0.11	1			
χ_{O10}	−0.19	−0.58	−0.51	0.92	−0.05	1		
r_{C8-O10}	−0.99	−0.92	−0.96	0.63	−0.48	0.31	1	
$r_{C8=O9}$	0.96	0.74	0.82	−0.31	0.46	0.04	−0.92	1

(B)

	$\sum n_{O9} \rightarrow (\sigma^*_{C-H/C})_{R1,R2}$	$\sum n_{X10} \rightarrow (\sigma^*_{C-H/C}/Ry^*_{C/H})_{R1,R2}$	$\sum^{O9=C8-X10}$	τ	χ_{C8}	χ_{N10}	r_{C8-N10}	$r_{C8=O9}$
$\sum n_{O9} \rightarrow (\sigma^*_{C-H/C})_{R1,R2}$	1							
$\sum n_{X10} \rightarrow (\sigma^*_{C-H/C}/Ry^*_{C/H})_{R1,R2}$	0.75	1						
$\sum^{O9=C8-X10}$	0.76	1	1					
τ	−0.59	−0.47	−0.47	1				
χ_{C8}	−0.31	−0.15	−0.16	0.28	1			
χ_{N10}	0.22	−0.17	0.15	−0.58	−0.13	1		
r_{C8-N10}	0.83	0.88	0.88	−0.31	0.09	−0.0	1	
$r_{C8=O9}$	0.31	−0.25	−0.23	−0.22	−0.57	0.3	−0.2	1

the variables $n_{O9} \rightarrow \sigma^*_{C-H}/\sigma^*_{C-C}$, $n_{X10} \rightarrow \sigma^*_{C-H}/\sigma^*_{C-C}/Ry^*_{C/H}$, and $\sum n_{O9/X10}/\sigma_{C4-H} \rightarrow \sigma^*_{C-H}/\sigma^*_{C-C}/Ry^*_{C/H}/\sigma^*_{N10-H}$ and the structural parameters τ, χ_{C8}, χ_{O10}, r_{C8-X10}, and $r_{C8=O9}$ (Table 8).

A significant linear correlation ($|R| > 0.7$) between τ, r_{C8-O10}, $r_{C8=O9}$, and NBO charges $n_{O10} \rightarrow \sigma^*_{C-H}/\sigma^*_{C-C}/Ry^*_{C/H}$ and $\sum n_{O9/O10} \rightarrow \sigma^*_{C-H}/\sigma^*_{C-C}/Ry^*_{C/H}/\sigma^*_{C4-H}$ in the group of structures with the O_9═C_8—O_{10} group quantitatively confirm our assumptions about why in Vpa and its derivatives τ, χ_{C8}, χ_{X10}, r_{C8-O10}, and $r_{C8=O9}$ do not show a behavior in agreement with the conventional model of the Theory of Resonance. We can remark that in Vpa and its derivatives, there are stabilizing interactions between the bonds of the R_1 and R_2 groups and the polar moiety which act not only to induce structural changes on the C_8═O_9 and C_8—O_{10} bonds and part of the R_1 and R_2 groups but also to regulate the planarity and the polarization of the π system in the O_9═C_8—X_{10} backbone.

Analyzing the information from Table 8A and B, it is possible to infer some reasons for the dominance of the cooperative delocalization effects of the π system in the O_9═C_8—O_{10} group regarding the importance of inductive and conjugative effects of the substituents on the O_9═C_8—N_{10} group. We understand that the low interrelationships of Table 8B with respect to those shown in Table 8A indicate that the O_9═C_8—N_{10} group is highly polarizable with respect to the O_9═C_8—O_{10} group, which can be explained by considering the difference in the electronic nature of N_{10} and O_{10} atoms and its response to the electronic effects of the environment. The high O_{10} electronegativity counteracts any inductive effect of R_2 in the direction of disrupting the cooperative delocalization effects of the π system and charge concentration on the electronegative atoms of the polar region. The opposite occurs in the group O_9═C_8—N_{10}; the low electronegativity of the N_{10} and its greater capacity to accommodate positive electrical charges contribute to the lability of the structural and electronic properties of this moiety to change with the electronic effects of its surroundings.

H. Proposed Structure−Activity Relationship. Considering the assumption that the manifestation of the activity of Vpa and its derivatives involves initial electrostatic interactions between the C═O group and the receptor active site, important differences in the atomic charge of atoms in the region O_9═C_8—N_{10} of the derivatives Suvpd and Chvpd of comparable anticonvulsant effect (PI_{Suvpd} = 19, PI_{Chvpd} = 17[4]) led us to propose that two types of anticonvulsant ligands can be obtained from Vpa from its functionalization to amide and esters.

According to the Q_{O9}, Q_{C8}, and Q_{X10} values, which can help us characterize the nature of the interaction of the O_9═C_8—X_{10} group in the specific receptor site, the optimization of the anticonvulsant activity in derivatives seems to be achieved with O_9═C_8—X_{10} slightly distorted from coplanarity and with a distinct reactivity toward electrophilic/nucleophilic attack. According to our calculations, derivatives resulting from significant activity against MES test (structures able to present activity at doses lower than 100 mg/kg) are those that show the following:

- an O_9═C_8—X_{10} moiety in a conformation almost coplanar with moderate reactivity toward nucleophilic attack and a low reactivity toward electrophilic attack. A polar region with this feature is achieved after the functionalization to an ester (Benvpa) or from secondary amides with bulky substituents of high affinity to lipophilic molecular fragments (aryl ring) with the capacity to conjugate the electron density of the amide group when oriented coplanar to the

dx.doi.org/10.1021/jp1081998 |J. Phys. Chem. A 2011, 115, 1686–1700

O_9═C_8—N_{10} skeleton (Bzvpd, Suvpd). In particular, the moderate reactivity of an electrophile of the amide group in Suvpd and the reduced reactivity of a nucleophile are consequences of the significant resonance between O_9═C_8—N_{10} and the —C_6H_4—SO_2NH_2 group promoted by the electron attractor —SO_2 group in a position para to the benzene ring.

- a coplanar O_9═C_8—X_{10} moiety with their two electron donor centers (C═O and >N:) of comparable reactivity toward the electrophilic attack. A polar region with these features is mainly achieved from the design of secondary amides with substituents whose inductive and/or conjugative effects stabilize the charge accumulated on the electronegative atoms, decrease the n_{N10} conjugation in the π system, and have moderately active reactivity of C_8 toward the nucleophilic attack. Within the set of structures under study, this type of distribution was obtained by joining to the polar region a cyclic —C_6H_{12} substituent (Chvpd) that interacts moderately with the donor−acceptor orbitals of the O_9═C_8—N_{10} moiety.

From Table 3 and taking into account that $Q_{O9} \cong Q_{N10}$ in Chvpd, we underline the following differences to compare the distributions of charge in Chvpd with respect to that predicted for Vpd (PI = 2.9, [4]): $Q_{O9,Chvpd} > Q_{O9,Vpd}$, $Q_{N10,Chvpd} < Q_{N10,Vpd}$, and $Q_{C8,Chvpd} > Q_{C8,Vpd}$

According to this interpretation and taking into account the charge distribution of O_9═C_8—X_{10} in the rest of the derivatives (see Table 3), we interpret that the low antiMES activity of Vpa could be related to the high positive charge on C_8 and the low negative charge on the O_9 atom and that structural changes that promote the polarization of the O_9═C_8—X_{10} group (Vpd) would favor the increase of antiMES activity (Vpd, $Q_{O9,Vpd} < Q_{O9,Vpa}$, $Q_{X10,Vpd} < Q_{X10,Vpa}$). Thus, derivatives with a pharmacological profile similar to that of the Vpd would result from structural changes that decrease mainly the polarization of the C_8—N_{10} bond (Ipvpd, Dmvpd, low value of Q_{N10}). In particular, we remark that the antiMES activity of the Etvpd could be greater than that observed for Vpd, Ipvpd, and Dmvpd due to having a C_8 center moderately active toward the nucleophilic attack [in Etvpd, $Q_{C8,Etvpd} < Q_{C8,Ipvpd,Dmvpd}$ due to $n_{N10} \rightarrow \pi^*_{C=O,Etvpd} > n_{N10} \rightarrow \pi^*_{C=O,Vpd,Ipvpd,Dmvpd}$].

On the basis of our formulations that point to the antiMES activity in the Vpa derivatives mainly modulated by the degree of polarization in the region O_9═C_8—X_{10}, we infer that the antiMES protection index of this new derivative could be close to 5 due to the fact that the Q_{O9}, Q_{C8}, and Q_{N10} values in Etvpd are comparable to those predicted for Aphvpd, that the biological activity of the Etavpd could be close to that observed for Chvpd (P.I <17) as we noticed that $(Q_{O9},Q_{C8},Q_{N10})_{Etavpd} \cong (Q_{O9},Q_{C8},Q_{N10})_{Chvpd}$, and that it is possible to infer the order of activity as Bzvpd < Suvpd because Bzvpd presents an electronic distribution comparable to that predicted for Suvpd (moderate reactivity of C_8 toward nucleophilic attack and reduced reactivity toward electrophilic attack in the C_8═O_9 and >N: units; $(|Q_{O9}|,|Q_{C8}|,|Q_{N10}|)_{Bzvpd} > (|Q_{O9}|,|Q_{C8}|,|Q_{N10}|)_{Suvpd}$).

Regarding the activity of the esters of Vpa, against the MES, test two peaks of maximum effect were observed, one in the period of 15−30 min and another at 4 h after intraperitoneal injection in adult albino mice (25−31 g).[43] The authors suggested that the pharmacological results indicate the existence of two chemical species capable of protecting against the MES test. Thus, under the supposition that the two maxima correspond to the protection due to the ester and the acid obtained from the in vivo hydrolysis of the ester, these authors reported that the Prvpa showed an early anticonvulsant effect minor to that observed for Vpa and Vpd without offering any explanation on such behavior.

On the basis of the data reported in this work (Table 3), we interpret that the lower anticonvulsant activity of Prvpa could be related to the high reactivity of C_8 as an electrophile ($Q_{C8,Prvpa} > Q_{C8,Vpa}$). This postulate is in agreement with our proposal that the optimization of the antiMES activity is achieved in derivatives with a C_8 of moderate reactivity toward a nucleophilic attack.

According to our last interpretation and comparing the charge distribution of O_9═C_8—O_{10} in Prvpa against the rest of the esters (Table 3), we infer that the biological activity of the Benvpa and Ispvpa would be somewhat greater than that observed for Prvpa because $Q_{C8,Benvpa,Ispvpa} < Q_{C8,Prvpa}$ and that Secvpa and Isbvpa would probably be less active than Prvpa because $Q_{C8,Secvpa,Isbvpa} > Q_{C8,Prvpa}$.

The results and interpretations reported here led us to undertake further investigations based on the analysis of the solvent effects on the second-order interactions between the polar region and the R_1 and R_2 substituents. Similarly, we will separately estimate the electronic effects of R_1 and R_2 on O_9═C_8—X_{10}, characterizing the intrinsic ability of R_1 and R_2 to disrupt the cooperative effects of delocalization of the π system, analyzing the orbital interactions of $n \rightarrow \sigma^*$, $\sigma \rightarrow \sigma^*$, $\sigma \rightarrow \pi^*$, and $\sigma \rightarrow Ry^*$ type. These results and structure−property quantitative relations between molecular properties of the polar region and the electronic hyperconjugative effects of R_1 and R_2 will be reported elsewhere in the near future.

CONCLUSIONS

A quantum mechanical description of the structural and electronic properties of valproic acid (Vpa) and its derivatives was performed by means of the natural bond orbital analysis, the electron localization function, and the quantum theory of atoms in molecules. From a systematic study of the electronic and topological properties of the polar R_1—C_8(═O_9)—$X_{10}R_2R_3$ fragment [where R_1 = —CH—$(CH_2$—CH_2—$CH_3)_2$, X_{10} = O and N, R_2 = —H, —CH_3, —CH_2—CH_3, —CH—$(CH_3)_2$, —$(CH_2)_2$—CH_3, —$(CH_2)_2$—$CH(CH_3)_2$, —C_6H_{11}, —$(CH_2)_2$—NH_2, —$C(CH_3)$·OH—$CH(CH_3)_2$, —CH·OH—$CH(CH_3)_2$, —CH_2—(C_6H_5), —$CH(CH_3)(C_6H_5)$, —CH—$(C_6H_5)_2$, and —C_6H_4·SO_2·NH_2, and R_3 = H and —CH_3, lp (lone pair electrons)], when considering the conformations of the mum energies of Vpa and their functional derivatives, we conclude(d) the following:

- The conventional model of the theory of resonance is not useful to explain the structural and electronic changes in the O_9═C_8—X_{10} moiety of Vpa and its derivatives. We found that the Winkler−Dunitz descriptors of the planarity (τ, χ_{C8}, and χ_{X10}) and the $r_{C8=O9}$ and $r_{C8—X10}$ bond lengths do not follow the expected trends; an increase of τ is accompanied by an increase in χ_C, χ_X, and $r_{C8—X10}$ and a decrease of $r_{C8=O9}$.
- The postulates of the theory of resonance are not satisfied when analyzing the nature of the interaction of the X_{10} atom with the carbonyl group in O_9═C_8—X_{10}. It can be seen by following the behavior of the natural atomic charges in the polar region that there is not a decrease in the polarization of the C_8═O_9 and C_8—X_{10} bonds and a reduction of the $n_{X10} \rightarrow \pi_{C8=O9}$ interaction with increasing τ.
- From the analysis of the structural characteristics of the molecular $[(O/N/C—H)_{R2}\cdots O_9]$, $[(C—H)_{R2}\cdots O_{10}]$,

$[(C_4—H)_{R1}\cdots H—N_{10}/O_{10}]$, and $[(C_4—H)_{R1}\cdots(H—C)_{R2}]$ subspaces focusing on the value of distances $r_{H\cdots O}$ and $r_{H\cdots H}$ and the improper angles $\alpha_{C8=O9\cdots(H)R2}$, $\alpha_{(O/N/C—H)R2\cdots O9}$, $\alpha_{C8—O10\cdots(H)R1}$, $\alpha_{(C4—H)R1\cdots O10}$, $\alpha_{N10—H\cdots(H)R1}$, $\alpha_{(C4—H)R1\cdots(H)}$, $\delta_{C8=O9\cdots(H—C/N/O)R2}$, $\delta_{C8—O10\cdots(H—C4)R1}$, $\delta_{N10—H\cdots(H—C4)R1}$, and $\delta_{(C4-H)R1\cdots(H—C/N)R2}$, we have found that the distortions of $O_9=C_8—X_{10}$ are accompanied by a three-dimensional arrangement of the units $C_8=O_9$ and $-\ddot{O}:_{10}/>N_{10}:$, with the C—H/C bonds of the substituents closing almost planar pseudorings of four, five, and six atoms at distances shorter than the sum of their van der Waals radii (2.122 Å $\leq r_{H\cdots O/N/H} \leq$ 2.668Å).

- From ELF, NBO, and AIM calculations, we have found that there are stabilizing intramolecular interactions of electrostatic origin in the subspaces $[(O/N/C—H)_{R1,R2}\cdots O_9]$, $[(C—H)_{R2}\cdots O_{10}]$, and $[(C_4—H)_{R1}\cdots H—N_{10}/O_{10}/C_{R2}]$ around the $O_9=C_8—X_{10}$ moiety.
- The charge delocalizations around the $O_9=C_8—X_{10}$ group described by the ELF and NBO calculations are qualitatively similar.
- From NBO calculations, the electronic delocalization in $[(O/N/C—H)_{R1,R2}\cdots O_9]$, $[(C—H)_{R2}\cdots O_{10}]$, and $[(C_4—H)_{R1}\cdots H—N_{10}/O_{10}/C_{R2}]$ occurs via two different mechanisms, interactions through the space (TSI) and interactions through the bonds (TBI).
- AIM calculations indicate intramolecular hydrogen bonds in structures where the donor−acceptor units exchange electrons via a TSI mechanism, forming quasi-planar hexa-atomic rings with dihedral angles $\alpha_{O9\cdots H—O}$, $\alpha_{O9\cdots H—C}$, and $\alpha_{H\cdots H—C}$ >100°.
- From an statistical analysis of the correlation between natural charge values and NBO delocalized charges on the $O_9=C_8—X_{10}$ moiety, we have found that 64.5−98.8% of the changes of the quantities, Q_{O9}, Q_{C8}, Q_{X10}, Q_{CR1}, and Q_{CR2} can be explained from the values of the transferred charges $n_{O9} \rightarrow \sigma^*_{C—H}/\sigma^*_{C—C}$, $n_{X10} \rightarrow \sigma^*_{C—H}/\sigma^*_{C—C}/Ry^*_{C/H}$, and $\sum n_{O9/X10}/\sigma_{C4—H} \rightarrow \sigma^*_{C—H}/\sigma^*_{C—C}/Ry^*_{C/H}/\sigma^*_{N10—H}$.
- The electron delocalization in $O_9=C_8—O_{10}$ follows a cooperative mechanism of charge redistribution that acts to counteract the effects of the decreased/increased charge on donor−acceptor units in the $[(O/N/C—H)_{R1,R2}\cdots O_9]$, $[(C—H)_{R2}\cdots O_{10}]$, and $[(C_4—H)_{R1}\cdots H—N_{10}/O_{10}/C_{R2}]$ regions.
- The electronic delocalization in the $O_9=C_8—X_{10}$ moiety will be dictated primarily by the charge redistribution mechanism on the electronegative atoms if X_{10} is very electronegative. On the other hand, if X_{10} can accommodate positive electric charges (N_{10}), changes in conformational and electronic properties of the polar region can only be rationalized by considering, in addition to the combined effects across space and through bonds in intramolecular regions $[(O/N/C—H)_{R1,R2}\cdots O_9]$, $[(C—H)_{R2}\cdots O_{10}]$, and $[(C_4—H)_{R1}\cdots H—N_{10}/O_{10}/C_{R2}]$, the intrinsic ability of R_1 and R_2 to disrupt the cooperative effects of delocalization of the π system.

■ ASSOCIATED CONTENT

Supporting Information. Relevant structural parameters, basin populations, donor−acceptor interactions, and value correlations. This material is available free of charge via the Internet at http://pubs.acs.org.

■ AUTHOR INFORMATION

Corresponding Author
*Phone/Fax: 54 221 4 259485.

■ ACKNOWLEDGMENT

N.C.C. acknowledges a fellowship from the Consejo Nacional de Investigaciones Científicas and Tecnologicas (CONICET); A.H.J. is a member of the Research Scientific Career (CIC-PBA), E.A.C. is a member of the Research Scientific Career CONICET, and R.M.L. acknowledges aid from Universidad de la Cuenca del Plata (Corrientes, Argentina) and facilities provided during the course of this work.

■ REFERENCES

(1) Malawska, B. *Curr. Topics Med. Chem.* **2005**, *5*, 69–85.
(2) Gatti, G.; Bonomi, I.; Jannuzzi, G.; Perucca, E. *Curr. Pharm. Des.* **2000**, *6*, 839–860.
(3) Nicolson, A.; Leach, J. P. *CNS Drugs* **2001**, *15*, 955–968.
(4) Tasso, S. M.; Moon, S. C.; Bruno-Blanch, L.; Estiú, G. L. *Bioorg. Med. Chem.* **2004**, *12*, 3857–3869.
(5) Tasso, S. M.; Bruno-Blanch, L.; Estiu, G. *J. Mol. Model.* **2001**, *7*, 231–239.
(6) Bialer, M.; Kadry, B.; Abdul-Hai, A.; Haj-Yehia, A.; Sterling, J.; Herzig, Y.; Shirvan, M. *Biopharm. Drug Dispos.* **1996**, *17*, 565–575.
(7) Hadad, S.; Vree, T.; Van der Kleijn, E.; Bialer, M. *J. Pharm. Sci.* **1992**, *81*, 1047–1050.
(8) Spiegelstein, O.; Kroetz, D. L.; Levy, R. H.; Yagen, B.; Hurst, S. I.; Levi, M.; Haj-Yehia, A.; Bialer, M. *Pharm. Res.* **2000**, *17*, 216–221.
(9) Avendaño, C. *Introducción a la Química Farmacéutica*; 1st ed.; McGraw-Hill/Interamericana: Madrid, España, 1993.
(10) Unverferth, K.; Engel, J.; Höfgen, N.; Rostock, A.; Günther, R.; Lankau, H. J.; Menzer, M.; Rolfs, A.; Liebscher, J.; Müler, B.; Hofmann, H. J. *J. Med. Chem.* **1998**, *41*, 63–73.
(11) Estrada, E.; Peña, A. *Bioorg. Med. Chem.* **2000**, *8*, 2755–2770.
(12) Gavernet, L.; Dominguez Cabrera, M. J.; Bruno-Blanch, L.; Estiu, G. *Bioorg. Med. Chem.* **2007**, *15*, 1556–1567.
(13) Tasso, S. M.; Bruno-Blanch, L.; Moon, S. C.; Estiú, G. L. *J. Mol. Struct.: THEOCHEM* **2000**, *504*, 229–240.
(14) Bello-Ramírez, A. M.; Carreón-Garabito, B. Y.; Nava-Ocampo, A. A. *Epilepsia* **2002**, *43* (5), 475–481.
(15) Hashemianzadeh, M.; Safarpour, M. A.; Gholamjani-Moghaddam, K.; Reza Mehdipour, A. *QSAR Comb. Sci.* **2008**, *27* (4), 469–474.
(16) Reed, A. E.; Curtiss, L. A.; Weinhold, F. A. *Chem. Rev.* **1988**, *88*, 899–926.
(17) Savin, A. *J. Mol. Struct.: THEOCHEM* **2005**, *727*, 127–131.
(18) Bader, R. F. W. *Atoms in Molecules: A Quantum Theory*; Oxford University Press: Oxford, U.K., 1990
(19) *HyperChem*, release 7.5 for Windows; Hypercube Inc.: Gainesville, FL, 2002.
(20) Peng, C.; Ayala, P. Y.; Schlegel, H. B.; Frisch, M. J. *J. Comput. Chem.* **1996**, *17*, 49–56.
(21) Becke, A. D. *J. Chem. Phys.* **1993**, *98*, 5648–5652.
(22) Lee, C.; Yang, W.; Parr, R. G. *Phys. Rev. B* **1988**, *37*, 785–789.
(23) Frisch, M. J.; Trucks, G. W.; Schlegel, H. B.; Scuseria, G. E.; Robb, M. A.; Cheeseman, J. R.; Montgomery, J. A., Jr.; Vreven, T.; Kudin, K. N.; Burant, J. C.; Millam, J. M.; Iyengar, S. S.; Tomasi, J.; Barone, V.; Mennucci, B.; Cossi, M.; Scalmani, G.; Rega, N.; Petersson, G. A.; Nakatsuji, H.; Hada, M.; Ehara, M.; Toyota, K.; Fukuda, R.; Hasegawa, J.; Ishida, M.; Nakajima, T.; Honda, Y.; Kitao, O.; Nakai, H.; Klene, M.; Li, X.; Knox, J. E.; Hratchian, H. P.; Cross, J. B.; Bakken, V.; Adamo, C.; Jaramillo, J.; Gomperts, R.; Stratmann, R. E.; Yazyev, O.; Austin, A. J.; Cammi, R.; Pomelli, C.; Ochterski, J. W.; Ayala, P. Y.; Morokuma, K.; Voth, G. A.; Salvador, P.; Dannenberg, J. J.; Zakrzewski, V. G.; Dapprich, S.; Daniels, A. D.; Strain, M. C.; Farkas, O.; Malick,

D. K.; Rabuck, A. D.; Raghavachari, K.; Foresman, J. B.; Ortiz, J. V.; Cui, Q.; Baboul, A. G.; Clifford, S.; Cioslowski, J.; Stefanov, B. B.; Liu, G.; Liashenko, A.; Piskorz, P.; Komaromi, I.; Martin, R. L.; Fox, D. J.; Keith, T.; Al-Laham, M. A.; Peng, C. Y.; Nanayakkara, A.; Challacombe, M.; Gill, P. M. W.; Johnson, B.; Chen, W.; Wong, M. W.; Gonzalez, C.; Pople, J. A. *Gaussian 03*, revision B.04; Gaussian, Inc.: Pittsburgh, PA, 2003.

(24) Glendening, E. D.; Reed, A. E.; Carpenter, J. A.; Weinhold, F. *NBO*, version 3.1. See http://www.gaussian.com/g_tech/g_ur/m_citation.htm.

(25) Becke, A.; Edgecombe, K. *J. Chem. Phys.* **1990**, *92*, 5397–5403.

(26) Noury, S.; Krokidis, X.; Fuster, F.; Silvi, B. *TopMod package*; 1997. http://www.lct.jussieu.fr/pagesperso/silvi/manual/node1.html.

(27) Biegler-König, F. W.; Bader, R. F. W.; Tang, T. H. *J. Comput. Chem.* **1982**, *3*, 317–328.

(28) Carey, F. A.; Sundberg, R. J. *Advanced Organic Chemistry. Part A: Structure and Mechanisms*, 5th ed.; Springer Science and Business Media, LLC: New York, 2007; pp 14−18.

(29) Pauling, L. *The Nature of the Chemical Bond*, 3rd ed.; Cornell University Press: Ithaca, NY, 1960.

(30) Krygowski, T. M.; Stepień, B. T. *Chem. Rev.* **2005**, *105*, 3482–3512.

(31) Dunitz, J. D. *X−Ray analysis of the structure of Organic Molecules*; Verlag Helvetica Chimica Acta: Switzerland, 1995.

(32) Glusker, J. P.; Lewis, M.; Rossi, M. *Crystal Structure Analysis for Chemists and Biologists (Methods in Stereochemical Analysis)*; Wiley-VCH: New York, 1994; pp 467−468.

(33) Silvi, B.; Savin, A. *Nature* **1994**, *371*, 683–686.

(34) Savin, A.; Silvi, S.; Colonna, F. *Can. J. Chem.* **1996**, *74*, 1088–1096.

(35) Poater, J.; Duran, M.; Solá, M.; Silvi, B. *Chem. Rev.* **2005**, *105*, 3911–3947.

(36) Weinhold, F. Landis, C. R. *Valency and Bonding. A Natural Bond Orbital Donor−Acceptor Perspective*; Cambridge University Press: New York, 2005.

(37) Jordan, K. D. Paddon-Row, M. N. In *Encyclopedia of Computational Chemistry*; P. v. R. Schleyer, Ed.; Wiley: Chichester, U.K., 1998; Vol. 2, pp 826−835.

(38) Alabugin, I. V.; Zeidan, T. A. *J. Am. Chem. Soc.* **2002**, *124* (12), 3175–3185.

(39) Bader, R. F. W. *J. Phys. Chem. A* **1998**, *102*, 7314–7323.

(40) Koch, U.; Popelier, P. L. *J. Phys. Chem.* **1995**, *99*, 9747–9754.

(41) Matta, C. F.; Hernández-Trujillo, J.; Tang, T. H.; Bader, R. F. W. *Chem. Eur. J.* **2003**, *9*, 1940–1951.

(42) Everitt, B. S. *The Cambridge Dictionary of Statistics*, 2nd ed.; Cambridge University Press: New York, 2002; R^2: Reduction factor of uncertainty associated with a variable response when the independent variable is known.

(43) Tasso, S. Ph.D. Thesis, Department of Biological Sciences, Faculty of Sciences, National University of La Plata, Argentine, 2003.